SYNTHESIS AND ANTIMICROBIAL ACTIVITY OF ZINC OXIDE NANORODS BY SOL-GEL ROUTE

A DISSERTATION

Submitted in partial fulfillment of the requirements for the award of the degree of

MASTER OF TECHNOLOGY

in

NANOTECHNOLOGY

By

DEVENDER NAIK JATOTH

CENTRE OF NANOTECHNOLOGY
INDIAN INSTITUTE OF TECHNOLOGY ROORKEE
ROORKEE -247 667 (INDIA)

JUNE, 2011

CANDIDATE'S DECLARATION

I hereby declare that the work presented as the dissertation thesis entitled "SYNTHESIS AND ANTIMICROBIAL ACTIVITY OF ZINC OXIDE NANORODS BY SOL-GEL ROUTE" in partial fulfillment of requirements for the award of the Master of Technology in Centre of Nanotechnology, Indian Institute of Technology Roorkee, India, is an authentic record of my own work carried out under the guidance of Dr. (Mrs.) VIJAYA AGRAWALA, Joint faculty, Centre of Nanotechnology and MMED, Indian Institute of Technology Roorkee, India

The matter embodied in this dissertation has not been submitted for the award of any other degree or diploma.

Date: 30.6.2011

Place: Roorkee

Devender Naik.

Devender Naik Jatoth

(09551004)

CERTIFICATE

This is to certify that the above statement made by the candidate is correct to the best of my knowledge and belief.

V Agarwala

(Dr. VIJAYA AGARWALA)
Joint faculty
Center of Nanotechnology
and
MMED
Indian Institute of Technology
Roorkee, Uttarakhand, India

ACKNOWLEDGEMENT

It gives me great pleasure to take this opportunity to thank and express my deep sense of gratitude to Dr. Vijaya Agarwala, Joint Faculty, Centre of Nanotechnology and Department of MME, Dr. R. C. Agarwala, Professor, Department of MME, and Dr. Naveen Kumar Navani, Department of Biotechnology, Indian Institute of Technology, Roorkee, for their invaluable guidance throughout the period of this dissertation work. Further, I am thankful to them for all the inspiration and motivation they inculcated in me.

I am obliged to Dr. Anil Kumar, Professor and Head, Centre of Nanotechnology for creating the right infrastructure and facilities conductive to my dissertation work. I express my sincere thanks to him for his kind help and moral support throughout this dissertation work.

I am also very thankful to Head of the Institute Instrumentation Centre for providing necessary facilities for this work.

Thanks are due to the entire staff of the department for their help and assistance, especially (Late) Mr. Arun Bhandari.

My special sincere heartfelt gratitude to my seniors especially Dr.(Mrs) Sulaxna Sharma, Ph.D., Mr. Sachin Tyagi and Mr. Devesh Devdutt Mishra, Research scholars, Department of MME, Mrs. Supriya and Mr. Tarun Sharma, Research scholars, Department of Biotechnology, Indian Institute of Technology.

I would like to express my gratitude to my parents; their blessings, motivation and inspiration have always provided me a high mental support and contributed in all possible way, in completion of this project work.

Devender Naik.

(DEVENDER NAIK JATOTH)

ABSTRACT

Zinc Oxide is a promising material with extensive application in semiconducting, piezolelectric, gas sensing and most importantly in medical use, due to its unique properties. Zinc Oxide nanostructured materials, whose structural elements have dimensions in the range of 1–100 nm, exhibit unique properties compared to the bulk material due to small dimensions and large surface area relative to volume. Because biological systems operate in the nanometer size range, nanostructured materials present possibilities for unique biological interactions.

Synthesis of nanostructures of Zinc Oxide can be attained by physical and chemical methods. In the present study, a novel, temperature dependant, size controllable synthesis of nanorods is achieved by a Sol Gel route. The bactericidal activity of synthesized nanorods, against *Escherichia coli, Micrococcus leuteus* and *Bacillus subtilis* is tested and found to be effective. Selectivity in toxicity is achieved by altering the capping agents, while retaining the morphology of synthesized nanorods. The synthesized nanorods were characterized by FESEM and EDAX analyses. The antibacterial activity was estimated by minimum inhibition concentration assay.

CONTENTS

LIST OF FIGURES

LIST OF TABLES

CHAPTER 1

INTRODUCTION

Antibacterial agents are of great importance in several industries, e.g., water disinfection, textiles, packaging, construction, medicine and food [1]. The organic compounds traditionally used for disinfection pose several disadvantages, including toxicity to the human body and sensitivity to high temperatures and pressures that are present in many industrial processes [1 and 2]. For these reasons, the interest in inorganic disinfectants such as metal oxides is increasing. These inorganic compounds present strong antibacterial activity at low concentrations. They are also much more stable in extreme conditions, considered as non-toxic, and some of them even contain mineral elements essential to the human body [3].

The key advantages of inorganic antimicrobial agents are improved safety and stability, as compared with organic antimicrobial agents. At present, most antibacterial inorganic materials are metallic nanoparticles and metal oxide nanoparticles such as zinc oxide. Nanoparticulate ZnO is a bactericide and inhibits both Gram-positive and Gram-negative bacteria. [4]

Although reports on synthesis of nanocrystalline ZnO are numerous, ZnO nanostructure continues to be of interest; it has been synthesized in the form of Nanoparticles by chemical precipitation [5], nanowires by solution-phase reaction [6], nanoparticles, nanosheets, and hexagonal nanopyramids by direct calcination [7], and nanoparticles, nanowires, nanobelts, nanorods, prismatic nanorods, nanosheets, nanoflowers, nanospheres, and hollow spheres by hydrothermal method recently. [8-11]

Among metal oxide powders, ZnO demonstrates significant growth inhibition of a broad spectrum of bacteria]. The suggested mechanism for the antibacterial activity of ZnO is based mainly on catalysis of formation of reactive oxygen species (ROS) from water and oxygen that disrupt the integrity of the bacterial membrane, although additional mechanisms have also been suggested. Since the catalysis of radical formation occurs on the particle surface, particles with larger surface area demonstrate stronger antibacterial

activity. Therefore, as the size of the ZnO particles decreases their antibacterial activity increases. [12]

Comprehensive data has not yet been obtained regarding ZnO nanorods. The nanorods produced via a hydrothermal route show more pronounced activity towards *Escherichia coli* than towards *Bacillus atrophaeus* (5M vs. 15M) [13]. The nanorods produced via a chemical route form flower like nanorods and are active against *Staphylococcus aureus*, E Coli. [14]

The synthesis of nanorods is generic as of now. This investigation aims at determining an exclusive method for synthesizing nanorods. The Sol-Gel route is commonly used for producing nanoscale materials; however, to isolate and strengthen a mechanism for synthesizing nanorods only, thereby attributing it to size controllable synthesis is the other of the major aims.

The purpose of size control is completely fulfilled only when its consequence is understood clearly. The relationship of structure of nanorods synthesized via the Sol-Gel mechanism with respect to the anti-microbial activity against few bacterial species is the other major aim. The size variation (growth and elongation of nanorods) is studied by varying reaction conditions and sonication times. The obtained nanorods are subsequently tested against bacteria.

CHAPTER 2

LITERATURE REVIEW

Nanostructured materials, whose structural elements have dimensions in the range of 1–100 nm, exhibit unique properties compared to the bulk material due to small dimensions and large surface area relative to volume [15]. These nanostructured materials are being investigated for use in an increasing number of applications such as microelectronics, sensor technology, semiconductors and cosmetics as well as medical applications such as biosensors, tissue engineering and drug delivery vehicles [16]. Because biological systems operate in the nanometer size range, nanostructured materials present possibilities for unique biological interactions. [17]

2.1 Synthesis of Zinc Oxide Nanoparticles

Although reports on synthesis of nanocrystalline ZnO are numerous, ZnO nanostructure continues to be of interest; it has been synthesized in the form of Nanoparticles by chemical precipitation [18], nanowires by solution-phase reaction [19], nanosheets, and hexagonal nanopyramids by direct calcination [20]. Nanowires, nanobelts, nanorods, prismatic nanorods, nanosheets, nanoflowers, nanospheres, and hollow spheres were synthesized by hydrothermal methods [21–25]. Karunakaran *et al.* [26] described a process in which ZnO Nanoparticles were prepared sonochemically; during sonication, NaOH was added gradually to a zinc salt solution and precipitation occurred immediately. The precipitate was dried under vacuum and calcinated at 500°C for 2 hours in a furnace. The ZnO nanoparticles prepared by the sonochemical route were shown to have bactericidal activity against E. coli.

A 'Green Synthesis' method was adopted by Razieh *et al.* [27] in which the ZnO nanofluids had been prepared by dispersing ZnO nanoparticles in glycerol as a base fluid, in the presence of ammonium citrate as a dispersant. The antibacterial activity of suspensions of ZnO nanofluids against E. coli had been evaluated by estimating the reduction ratio of the bacteria treated with ZnO. Toral *et al.* synthesized Zinc Oxide

nanorods by a solution-based hydrothermal growth method. To arrest the nanorods growth, the substrates were removed from solution, rinsed with de-ionized water and dried in air at room temperature. [28]

Tam *et al.* show that ZnO nanorod arrays fabricated by a hydrothermal method have an advantage of low growth temperature (90°C) [29-32] and a variety of possible substrates. This fabrication process is inexpensive and environmentally friendly. The nanorod arrays were prepared from equimolar aqueous solutions of zinc nitrate hydrate and hexamethylene tetramine by a hydrodermal method. ZnO exhibited antibacterial activity against both E. coli and *Bacillus atrophaeus.* [33]

Bulk ZnO samples are grown by various techniques. A possibility to grow ZnO by gas transport is given by the following reactions:

$ZnO + H_2 \rightarrow Zn + H_2O$ (1)

$2Zn + O_2 \rightarrow 2ZnO$ (2)

Sometimes graphite is used for the reduction of zinc instead of H_2. Pressed or sintered samples of high-purity ZnO powder are reduced to Zinc vapor at elevated temperatures by hydrogen (or the addition of graphite) which is transported with a flow of inert gas like N_2. The zinc vapor is then oxidized in a region of lower temperature under the admission of oxygen or air. Platelets and particularly beautiful hexagonal needles can be grown with diameters up to several mm. [34]

A number of investigations on the synthesis of ZnO nanoparticles have been reported in the literature. There have been several reports of solution-phase synthesis of ZnO nanoparticles at low temperature. The synthesis of these particles is mainly based on the alcoholic hydrolysis of zinc precursors [34, 35], hydrothermal methods [36] and electrochemical routes [37]. Among these techniques, the hydrolysis route is very attractive because it is relatively easy to perform and allows us to tailor the morphology of the particles by controlling the rate of hydrolysis and condensation reactions. Hossain *et al.* [38] had obtained nanobelts of ZnO of length 700 mm using refluxing technique. Several workers have used capping agent such as vinyl pyridine (PVP), polyethylene glycol (PEG), etc. to stop particle agglomeration and obtained nanoparticles of size less

than 5 nm. One hydrothermal method commonly used to synthesize ZnO for more than 50 years[39, 40] is to grow single crystals (generally > 5 cm) by slow dissolution of ZnO powder held at a higher temperature relative to a ZnO "seed" crystal held at a lower temperature, all within a high temperature (generally > 300 °C) autoclave. Generally, "mineralizers" such as KOH, NaOH, and NH_4OH are used to increase the solubility of ZnO powder and thus to increase the growth rate of the single crystals. A second hydrothermal method uses a zinc salt such as $ZnCl_2$, $Zn(NO_3)_2$ or $Zn(CH_3COO)_2$ to synthesize ZnO powders with different particle morphologies at lower temperatures (80 °C to 200 °C).

Much research has been focused on the preparation and the properties of ZnO nanocrystals; however, little of it dealt with the pH effect of the sol on the crystallite size of ZnO powder. For instance, Li *et al.* [41] concluded that the solution conditions have a certain effect on the particle size of ZnO powders under hydrothermal conditions. Zhang *et al.* [42] found that the pH value can change the quantity of ZnO nuclei and of growth units. Lu and Yeh found that the characteristics of ZnO powder profoundly depend on the pH of the starting solutions. In addition the crystallinity and particle size of ZnO powder increase with a rise in the pH of solution. [43]

2.1.1 Mechanochemical synthesis

Milling of precursor powders leads to the formation of a nanoscale composite structure of the starting materials that react during milling or subsequent heat treatment to form a mixture of separated nanocrystals of the desired phase within a soluble salt matrix. The separation of the nanoparticles occurs due to existence of NaCl that prevents the subsequent agglomeration ZnO nanoparticles during calcination. Removal of the salt matrix is usually carried out through simple washing. For example, ultrafine ZnO powder was synthesized by the milling and subsequent heat treatment of a $ZnCl_2$, NaCl and Na_2CO_3 powder mixture. Removal of the NaCl with a simple washing process resulted in separated ZnO particles [44 - 46].

The starting materials were anhydrous $ZnCl_2$ granules, Na_2CO_3 powder and NaCl. All the starting materials were dried in air at 150°C. A stoichiometric mixture of the starting materials was milled corresponding to the following reaction equation:

$$ZnCl_2+Na_2CO_3+ 8NaCl \rightarrow ZnCO_3+ 10NaCl \quad (3)$$

NaCl was added to the reactants so that the volume ratio of the $ZnCO_3$: NaCl in the product phase was 1:10. The NaCl was used as an inert diluent and added to the starting powders. The mixture of starting powders was milled in a ball mill with zirconia balls of 10mm in diameter and 250 rpm .The precursor was calcined at 400°C in air in a porcelain crucible to prepare the ZnO nanoparticles. Since the mechanochemically formed $ZnCO_3$ nanoparticles were isolated in the NaCl matrix, sintering of the ZnO powder did not occur during heat treatment. Removal of the salt by-product was carried out by washing the powder with de-ionised water. The washed powder was dried in a spray drier.

2.1.2 Sol-gel method of synthesis for Nanoparticles:

Sivakumar *et al.* used zinc acetate dihydrate as a precursor and 0.2M NaOH for hydrolysis to produce flower like nanorods by a sol gel mechanism. The antibacterial activity of cotton loaded with these nanorods was tested against three organisms namely *Staphylococcus aureus*, *Escherichia coli* and *Pseudomonas aeruginosa* in terms of live bacterial load, as measured by the colony forming units (CFU), adhered on the cotton surface. More than 99% reduction in bacterial load was observed against all three organisms. [47]

A standard procedure had been developed by Lu and Yeh [24] to produce Nanoparticles via the sol gel method. The ZnO sols were prepared by dissolving zinc acetate dihydrate (99.5% $(CH_3COO)_2Zn{\cdot}2H_2O$, Merck) in methanol at room temperature. The sol prepared was found to be stable and transparent with no precipitate or turbidity. ZnO powders were prepared by varying the pH value of sol from 6 to 11. The clear solution was filtered through micron filter paper. The resulting transparent filterate was kept for 48 hours to complete the gelation and hydrolysis processes. During this period of time, white ZnO precipitates slowly crystallized and settled down in the bottom of the flask. The size and activity of solvent have obvious influence on the reacting progress and product. Methanol has smaller size and a more active –OH and $–OCH_3$ groups. Methanol reacts more easily.

to form a polymer precursor with a higher polymerization degree, which is required to convert sol into gel [48]. These zinc hydroxide splits into Zn^{2+} cation and OH^- anion according to reactions and followed by polymerization of hydroxyl complex to form ''Zn–O–Zn'' bridges and finally transformed into ZnO. [49]

When the concentration of OH^-, i.e. pH is low, the growth of ZnO particle does not proceed because of the lack of $Zn(OH)_2$ formation in the solution Therefore, in sol gel technique there is a threshold pH level above which the nanostructure may be formed. In this study, the growth of ZnO nanoparticles in zinc acetate solution was observed from a solution having pH of 7. Since pH controls the rate of ZnO formation, it affects the size and their way of combination to get stable state. As the freshly formed nuclei in the solution are unstable, it has a tendency to grow into larger particles.

2.1.3 Sol Gel method of synthesis for nanorods

Taking queue from the procedure described by Lu and Yeh [24], in this work ZnO powder was synthesized using sol gel route. Zinc Nitrate Hexahydrate (99.5% Zn $(NO_3)_2 \cdot 6H_2O$, Merck) was used as a precursor due to easier control of hydrolysis. The 1M **Sol** formed by dissolution of 5.9grams of zinc salt in 20ml of water was found to be stable and transparent with no precipitate or turbidity. For the formation of the **Gel** an alcohol base (methanol) is added. A suitable capping agent such as Ethylenediamine or Citric Acid Monohydrate is added prior to the hydrolysis and gelation process. The gelation is initiated by hydrolysis of the zinc salt by drop wise addition of 10M NaOH solution under constant stirring conditions. Stoichiometrically, when enough amount of NaOH is provided for the hydrolysis of zinc from zinc salt, a milky white and turbid **"Gel"** is observed which retains its turbidity even upon magnetic stirring at 200 r.p.m.

The hydrolyzed zinc ions act as sites of nucleation and subsequently zinc hydroxide is accumulated and crystal growth occurs. The presence of capping agent restricts this growth of zinc hydroxide after a certain limit. This gel formation is facilitated by allowing 2 hours of magnetic stirring at 200r.p.m. However, to separate the agglomerates formed by these nanosized zinc hydroxide nanorods, more energy is required. An ultrasonic vibrator is employed for providing this high energy for another 2 hours and samples are collected at regular time intervals.

After Sonication, the sample is allowed to settle under gravity. After about 1 hour, a clear cake of precipitate is observed. The supernatant is decanted and the precipitate is washed repeatedly with distilled water to remove the excess NaOH. The sample is now calcinated at 150°C overnight to convert the ZnOH into ZnO. The calcination process also serves for removal of water after washing.

The growth of nanosized ZnO from zinc nitrate hexahydrate precursor using sol gel process generally undergoes four stages, such as solvation, hydrolysis, polymerization and transformation into ZnO. The zinc nitrate hexahydrate precursor was first solvated in methanol, and then hydrolyzed, regarded as removal of the intercalated nitrate ions and results in a colloidal–gel of zinc hydroxide (Eq. (4)). The size and activity of solvent have obvious influence on the reacting progress and product. Methanol has smaller size and a more active –OH and –OCH3 groups. Methanol can react more easily to form a polymer precursor with a higher polymerization degree, which is required to convert sol into gel [28]. These zinc hydroxide splits into Zn^2+ cation and OH¬- anion according to reactions (Eq.(5)) and followed by polymerization of hydroxyl complex to form ''Zn–O–Zn'' bridges and finally transformed into ZnO (Eq. (6)) [29]

$$Zn(NO_3)_2 \cdot 6H2O + CH_3OH \longrightarrow Zn(OCH_3)^{2}\neg + 2CH_3COONa + 2H_2O \quad (4)$$

$$Zn(OCH_3)^{2+}\ NaOH \longrightarrow Zn(OH)^{2+} + 2CH_3{}^{2+} \quad (5)$$

$$Zn(OH)_2{}^{2+} \longrightarrow ZnO + H_2O + 2OH^- \quad (6)$$

When the concentration of OH-, i.e. pH is low, the growth of ZnO particle does not proceed because of the lack of $Zn(OH)_2$ formation in the solution. Two mechanisms govern the crystal formation and growth.

(1) Fusion of one primary crystallite (10 nm) into another.

(2) Aggregation of the primary crystallites (more than 10 nm).

The first mechanism will yield a large particle giving crystallite size of micrometer scale (mm). The second route will result a bigger particle consisting of primary (10 nm) subunits with porosity. In the present work it appears that the aggregation is the dominant mechanism which occurred during the crystallization of gel network leading to macroscopic ZnO nanorods.

2.1.4 Factors affecting the morphology of Nanorods

In this work, various factors are found to have control over the morphology of the final powder of nanorods. It begins at the gelation stage where use of excessive capping agent is not conducive to formation of nanorods. Ultra sonication of the Gel to restrict agglomeration helps only in isolating and preventing nanorods from sticking to each other. Most importantly, the calcination temperature and time for conversion of ZnOH to ZnO nanorods is the detrimental step. As evident from the data (fig 5.3 and fig 5.4), a calcination temperature of 150°C is found to be optimum for production of nanorods which retain their desired morphology as well as antibacterial nature. However, when Citric Acid Monohydrate is used as capping agent, a calcination temperature of 170°C for 5 hours is found optimal.

2.2 Antibacterial Activity

ZnO is an environmentally friendly material and has little toxicity, which is why it is widely used as an active ingredient for dermatological applications in creams, lotions and ointments on account of its antibacterial properties. The antibacterial properties were found in both microscale and nanoscale formulations. [50] The theme of particle-induced reactive-oxygen-species (ROS) production and oxidative injury inside bacterial cells has become an established paradigm underlying the ZnO antibacterial mechanism. [51], [52]

An important aspect of the use of ZnO as antibacterial agent is the requirement that the particles are not toxic to human cells (Huang *et al.*., 2008; Nair *et al.*., 2008). Although the exact mechanism has not yet been clearly elucidated, the suggested mechanisms include the role of reactive oxygen species (ROS) generated on the surface of the particles (Applerot *et al.*., 2009; Sawai *et al.*., 1996, 1997, 1998), zinc ion release (Yang & Xie, 2006), membrane dysfunction (Yang & Xie, 2006; Zhang, Jiang, Ding, Povey, & York, 2007), and nanoparticle internalization (Brayner *et al.*., 2006). [47]

Nanoparticles of ZnO are also known for their anti-bacterial activity against both gram-negative and gram-positive bacteria. [17] In vitro antibacterial activity and efficiency of regular zinc oxides (for examples, high-purity fine powders commercially available) were also carefully examined. Sawai and Yoshikawa [53] reported that after quantitative evaluation of antibacterial activities of some metal oxide powders (ZnO, MgO and CaO), ZnO was the most effective for *Staphylococcus aureus*, which might be due to strong affinity to their cells. Sawai *et al.* have investigated the antibacterial behaviors related of ZnO-based substances intensively, i.e., ZnO–CaO solid solutions, carbon powders containing ZnO [12], mixtures of ZnO and MgO powders, developing a quantitative evaluation method, and identification of reactive oxygen species (ROS) generated from ZnO. The sustainable antibacterial activity of thus fabricated ZnO ceramics might be originated from the generation of super-oxide anion ($-O_2^-$). [54]

The nanorod arrays were prepared from equimolar aqueous solutions of zinc nitrate hydrate and hexamethylene tetramine by a hydrodermal method. ZnO exhibited antibacterial activity against both E. coli and B. atrophaeus, but it was considerably more effective in the latter case (at 15 mM vs. 5 mM concentration, respectively, showing zero viable cell count). For both organisms, damage of the cell membranes was found, and the effect was more pronounced for B. atrophaeus. [55]

Sivakumar *et al.* carried out experiments with cotton loaded with flower like ZnO nanorods and it was shown that 99.99% reduction in bacterial adhesion on coated cloth against *Staphylococcus aureus*, *Escherichia coli* and *Pseudomonas aeruginosa*. Backlight studies showed that the coating activity exhibit membrane disruption activity which is an added advantage. [56]

Aqueous suspensions of ZnO nanoparticles (ZnO nanofluids) are the preferred formulation for using the antibacterial agent in liquid phases and for the incorporation of the nanoparticles in different commercial products. However, ZnO nanoparticles in aqueous media tend to aggregate into large flocculates, due to their hydrophobic nature, and thus do not interact with microorganisms effectively. Tamar *et al.* in their study,

showed that zinc oxide was combined with iron oxide to produce magnetic composite nanoparticles with improved colloidal aqueous stability, together with adequate antibacterial activity. [57]

In this work, dry powders of ZnO nanorods are tested against both Gram positive and Gram negative bacterial species. The powders are placed on the lawn of actively growing bacteria (as a spot) and bactericidal activity is looked for in the form of zone of inhibition. If zone of inhibition is found, these powders are tested further to determine quantitatively the amount of bactericidal activity via minimum inhibitory concentration tests.

2.3 Applications of ZnO

In recent years, the use of inorganic antimicrobial agents has been attracted interest for the control of microbes. The key advantages of inorganic antimicrobial agents are improved safety and stability, as compared with organic antimicrobial agents. [58] At present, most antibacterial inorganic materials are metallic nanoparticles [59-61] and metal oxide nanoparticles such as zinc oxide. [62]

2.4.1 Present applications

Zinc oxide (ZnO) has been investigated in a number of biomedical applications and surfaces presenting well-controlled nanorod structures of ZnO have recently been developed. Toral *et al.* showed that a decrease in viable macrophage numbers when ZnO substrates were present in the media confirmed the role of ZnO substrate dissolution. [17] Other applications concern medicine or cosmetics. ZnO is used as a UV-blocker in sun lotions or as an additive to human and animal food. Furthermore, it is used as one component of mixed oxide varistors, devices that allow voltage limiting. [63]

ZnO nanoparticles strongly inhibit the action of pathogenic microbes when used in small concentrations. Moreover these are durable and show great selectivity and heat resistance. [64, 65] ZnO nanoparticles possess antibacterial and antifungal activities at lower concentrations; therefore, the thin coatings of such nanoparticles can be used for the preparation of microbial resistant articles. Moreover, use of ZnO nanoparticles as

antifungal agent does not affect the soil fertility in comparison to traditional antifungal agents. [66]

2.4.2 Future applications:

The coating of nanoparticles with biomolecules, oil, pigments polymers, plastics, etc., with the help of suitable binders and co-binders has been reported as well. Less attention has been paid to nanoparticles of ZnO as coatings, in spite of their known technological applications. [67]

The most common pathogens in hospitals include staphylococci (especially Staphylococcus aureus), Pseudomonas, and *Escherichia coli*. According to a 2006 report, nosocomial infections are estimated to occur in at least 5% of all patients hospitalized (Nguyen, 2006). Direct contact between host and infected person is recognized to be the most important mode of transmission of nosocomial infection (Borkow & Gabbay, 2008) and the contaminated objects predominantly include cloth materials such as bed linen, towel and clothing. [14] More Research into these areas can be foreseen in the near future.

CHAPTER 3

FORMULATION OF PROBLEM

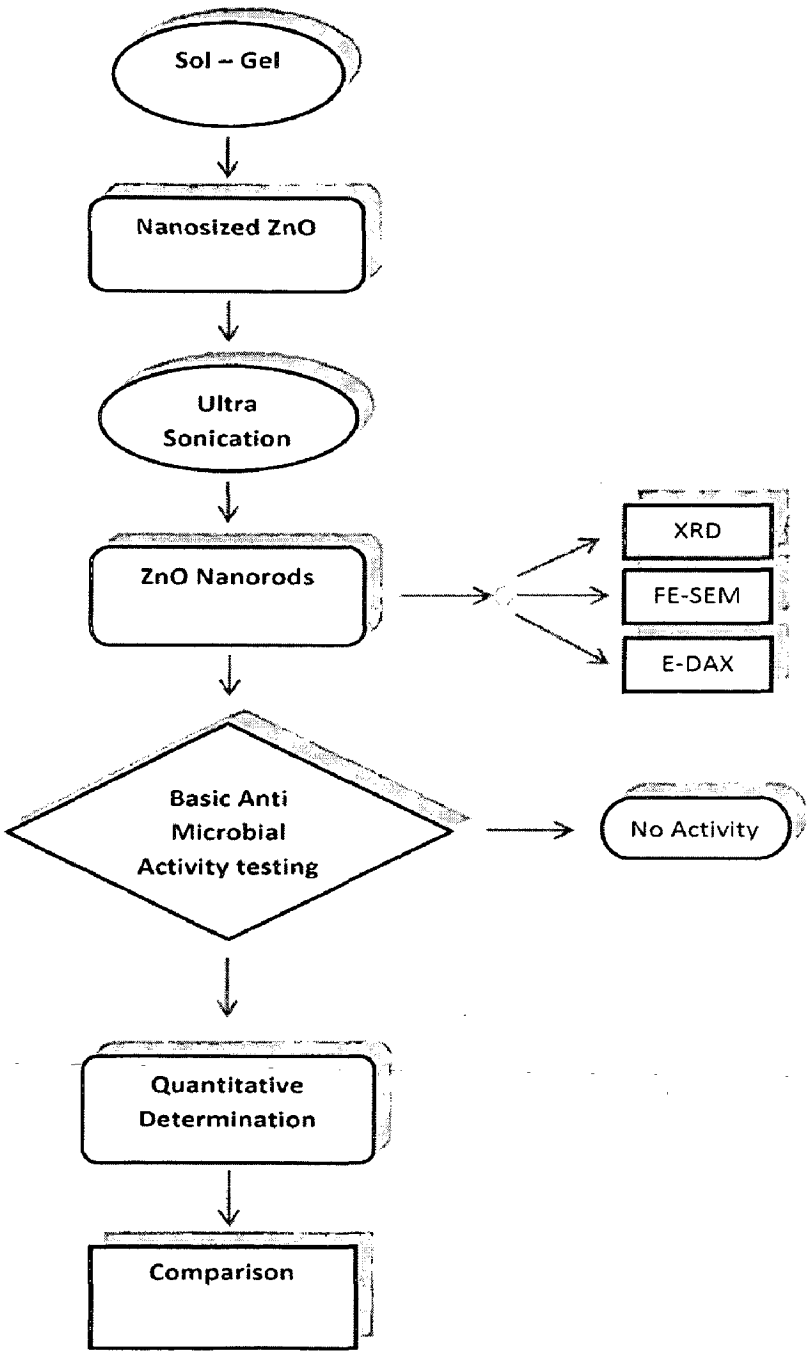

Figure 3.1: Flow chart of processes involved in the experiment

CHAPTER 4

EXPERIMENTAL WORK

4.1 Materials and Instruments used

The following materials and equipment were made use of in the course of this experiment.

4.1.1 Chemical salts and Reagents used

- Zinc Nitrate Hexahydrate (Sigma–Aldrich)
- Zinc acetate dehydrate (Merck)
- Ethylenediamine (Sigma–Aldrich)
- Citric Acid Monohydrate (Sigma–Aldrich)
- Ethanol (Changsu Yang Yuan)
- Sodium Hydroxide (J. T. Baker)
- Methanol (Rankem)
- Tri sodium citrate (Merck)
- Agar Agar (HiMedia)
- LB Broth (HiMedia)

4.1.2 Instruments and Equipment used

- Heating Oven (Fig. 4.1(a))
- Magnetic stirrer (Make REMI)
- Ultra Sonicator (Sonics, 500 Watts, 20KHz , Fig. 4.1(b))
- Bruker X-8, X-Ray diffraction instrument (Fig. 4.1(c))
- FEI Quanta200f for FESEM and EDAX
- Elix Millipore for Distilled water (Fig. 4.1 (d))
- Laminar Hood for biological exposure and inoculums transfer (Fig. 4.1(e))
- Digital controlled autoclave for decontamination (Fig. 4.1(f))

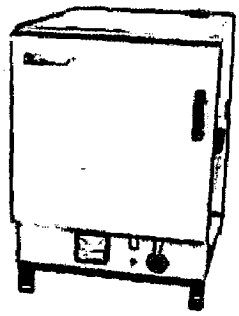

(a)

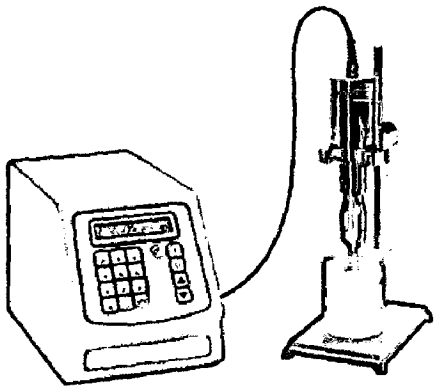

(b)

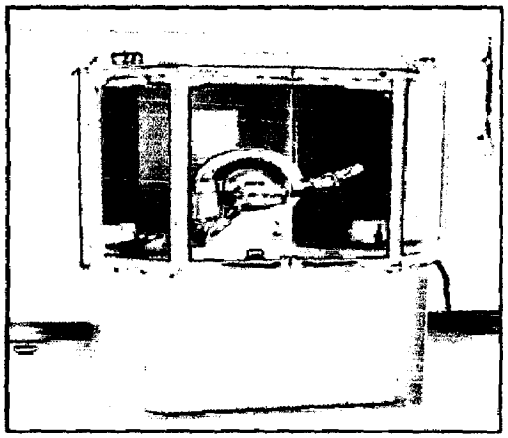

(c)

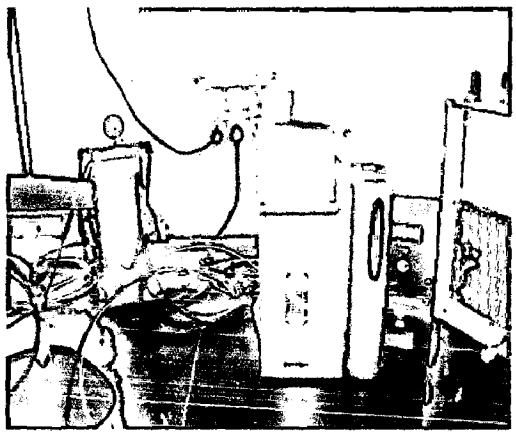

(d)

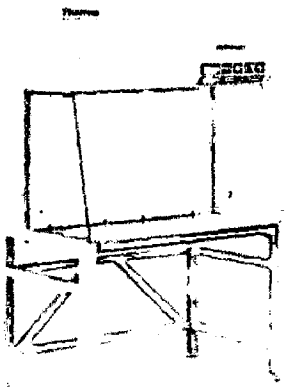

(e)

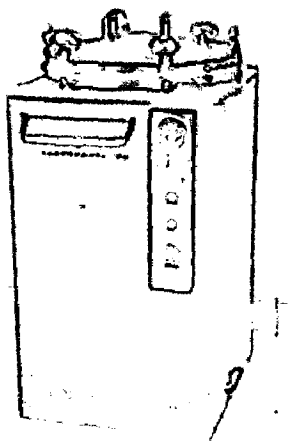

(f)

Figure 4.1 Instruments used: (a) Digital controlled Heating Oven (b) Ultrasonicator (c) Bruker D-8 Advance (d) Elix Milipore for Distilled water (e) Laminar Hood (f) Autoclave

4.2 Synthesis of ZnO nanorods by Sol-Gel method

4.2.1 With EDA as capping agent

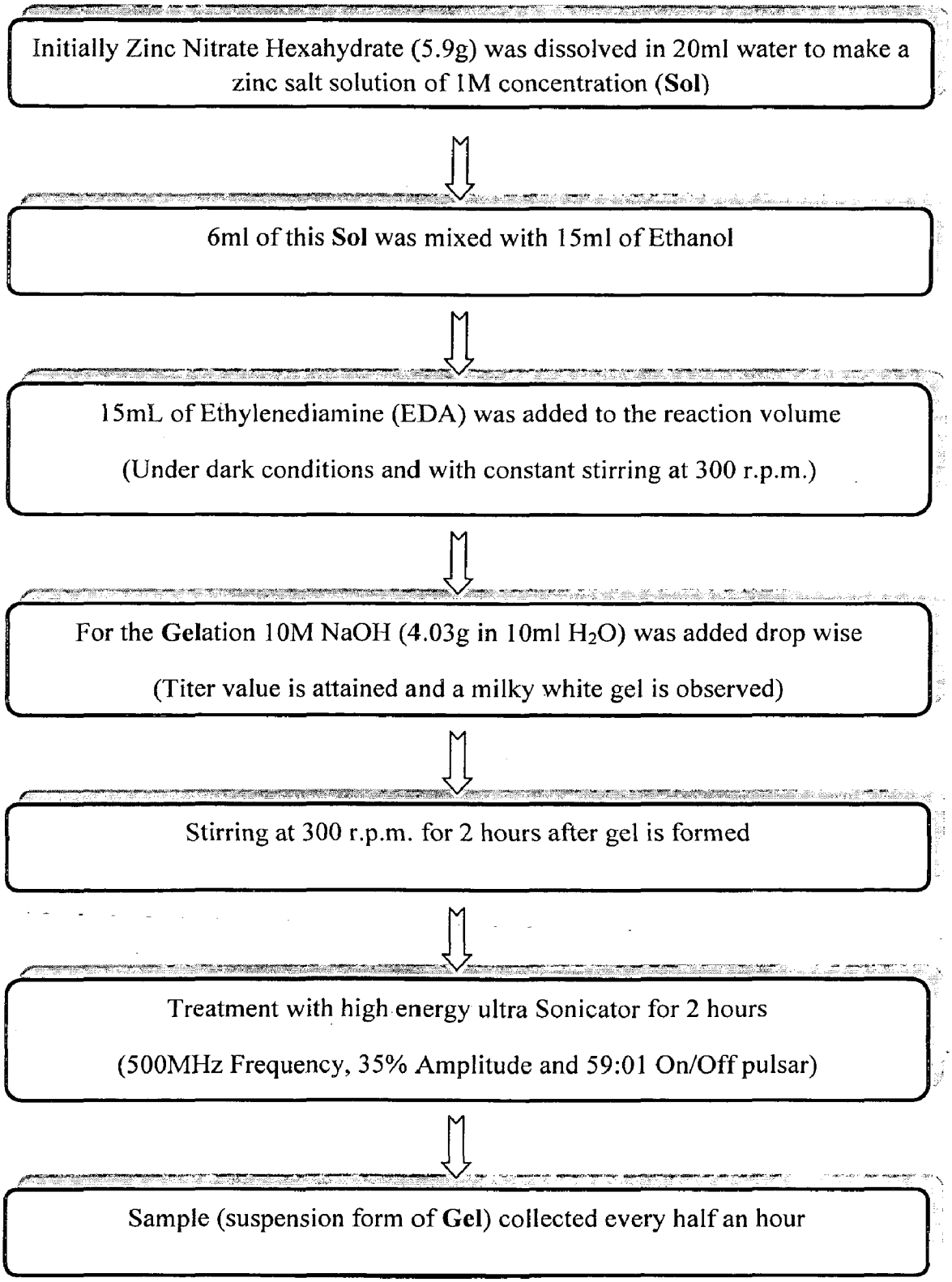

4.2.2 With Citric Acid Monohydrate as capping agent

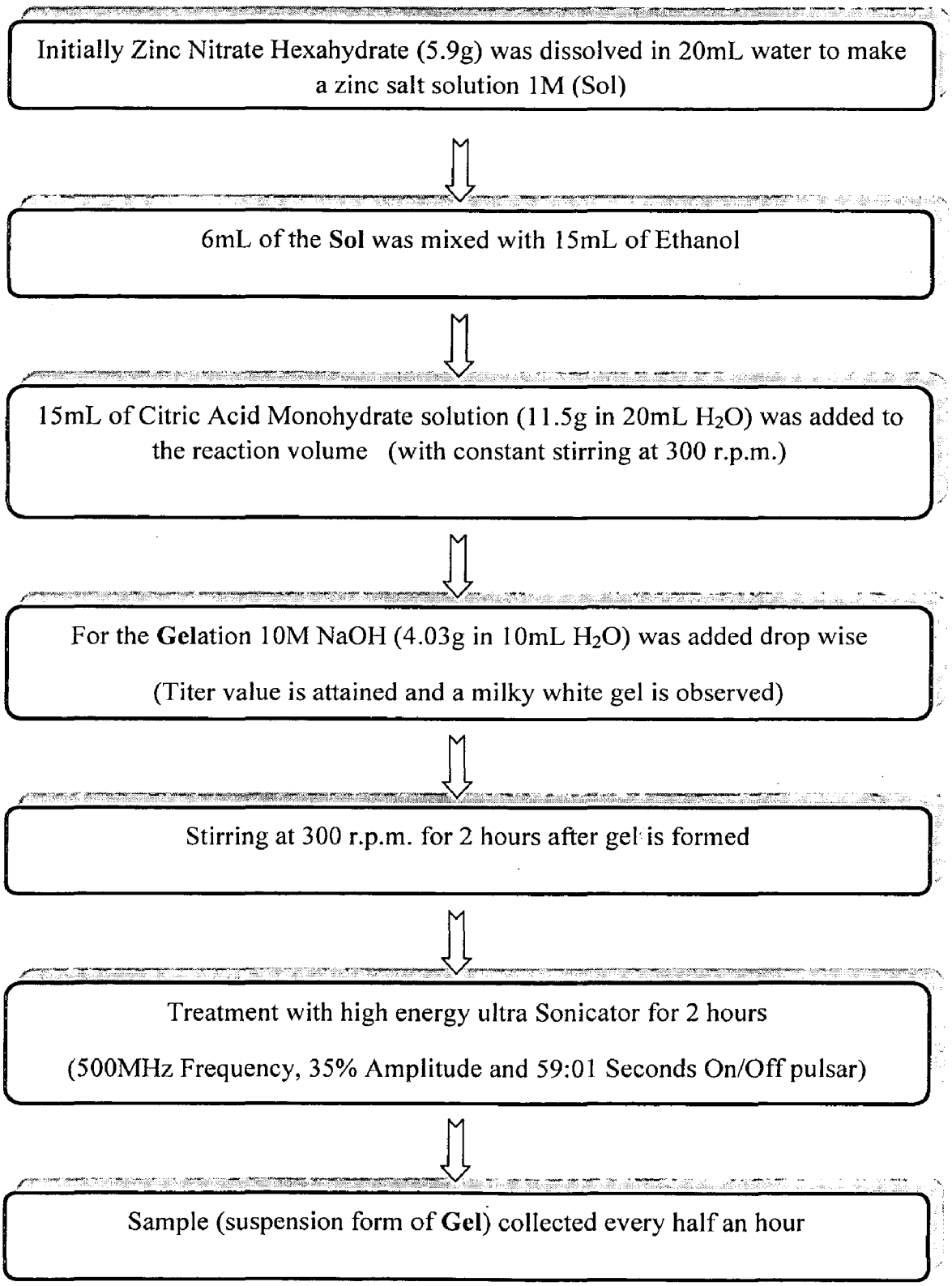

The above processes were done with Methanol as well, in place of Ethanol.

4.3 Drying and retrieval of ZnO Nanorods

4.3.1 By Pre-drying washing

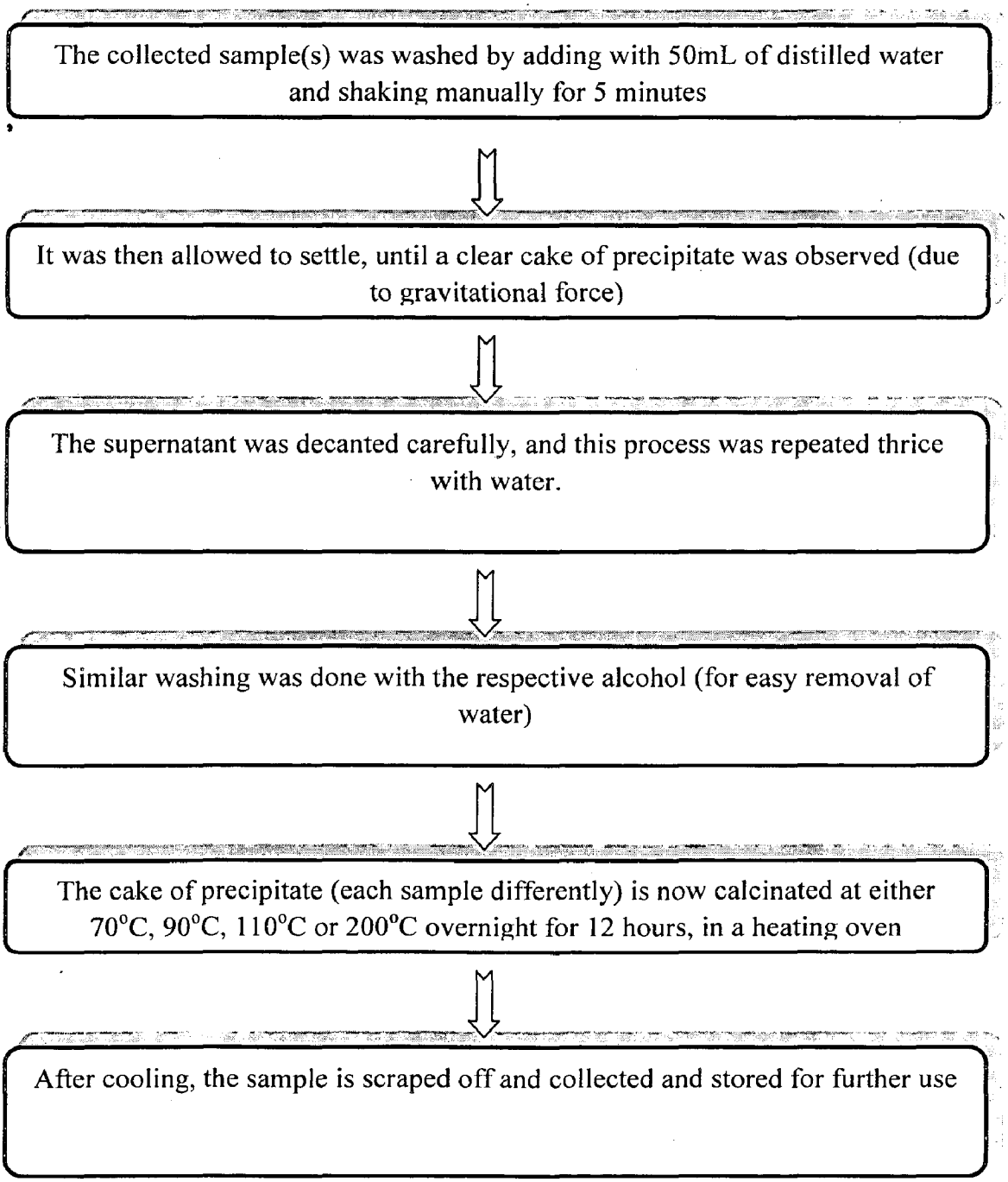

4.3.2 By Post-drying washing

After Sonication the sample(s) was allowed to settle until a clear cake of the precipitate is observed (due to gravitational force)

The supernatant was decanted carefully; the precipitate was dried at 50°C for two hours (for removal of water)

The cake of precipitate (each sample differently) is now calcinated at either 70°C, 90°C, 110°C and 200°C overnight for 12 hours

After cooling, the sample is scraped off and collected, and washed with 50mL distilled water.

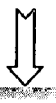

The sample was allowed to settle, until a clear cake of precipitate was observed (due to gravitational force)

The washing process is repeated thrice with distilled water, and then allowed to dry at 60°C

4.4 Preliminary (Qualitative) Anti-microbial activity determination

The preliminary activity determination tests (also know as plus-minus tests) were done by allowing bacteria to grow normally in predetermined laboratory conditions, and also by subjecting to ZnO nanorods in the powder form. On comparison of the above two Petri plates, the presence of a **zone of inhibition** indicates the anti microbial nature, which would have not existed if the bacteria did not experience any adverse affects by the presence of the ZnO Nanorods.

4.4.1 Preparation of Inoculums

1. Single isolated colony from a fresh agar plate culture of bacterial strain was inoculated into a tube containing 5ml Lb broth media.
2. It was incubated at 37 °C, 200 rpm for 12h.
3. It was then subcultured(1%) into fresh 5 ml LB broth medium and incubated at 37 °C, 200 rpm till OD reached 0-5-0.7 at 600nm.
4. The cells were diluted 10^4 times in LB broth media for 96 well plate assay.

4.4.2 Preparation of Petri plates

For 200mL of growth media:

- 5g of LB broth was dissolved in distilled water
- 2 grams of Agar (solidifying agent) was added to the above solution.
- This solution was then autoclaved at 100°C at 125lbs for 15 minutes.
- The solution is allowed to cool and poured into petri plates before it solidifies completely.(approximately 80 mL in a standard petri plate)
- The petri plates are tightly sealed with paraffin wax tape strips and stored for further use.
- For spot on lawn assay, the 1% subculture of bacteria is now streaked onto the solidified growth medium with the help of autoclaved spreaders.

4.4.3 Qualitative Activity Determination

- After spreading the bacterium on the solidified media, a spatula of the powdery samples (nanorods) was placed distant form each other almost along the circumference of the Petri dish.
- The Petri dish was inverted and shaken to make sure no spillage of the powdery nanorods occurred.
- The Petri dish was then covered and sealed with paraffin thin film.
- A replica was also done to ensure corroboration.
- A "blank" Petri dish was inoculated for establishing the activity of the anti-microbial agent by mere comparison.
- The 'loaded' Petri plates are now incubated as per the standard growth demands of the respective bacteria.
    - For E.Coli ATCC strain(Gram Negative) 12 hour incubation at room temperature
    - For *Bacillus subtilis* strain 12 hour incubation at 37°C.
    - For *Micrococcus leuteus* strain 12 hour incubation at 37°C.

4.5 Quantitative Activity Determination

A standard MIC Assay is the most direct and reliable quantitative measure of the activity of the antimicrobial agent. Here, the exact critical amount of antimicrobial agent required to kill a specific amount of bacteria can be established.

4.5.1 MIC Assay

Serial dilutions in 96 well plate

1. The dilutions were carried out in duplicates for each sample of the bacterial extract to be tested.
2. The 12^{th} well in each row contains the highest conc. (vol/vol) of the bacterial extract i.e. 500ul/ml. 200ul of the bacterial extract was added to the 12^{th} well.
3. 100ul of LB broth was added to remaining wells.

4. For serial dilution, 100ul supernatant from 12^{th} well was transferred into 11^{th} well.
5. The serial dilution was continued similarly upto 3^{rd} welland 100ul of the contents from 3^{rd} well were transferred directly to the 1^{st} well (as 2^{nd} well is used as positive control i.e without bacterial extract).
6. 100ul of the diluted e.coli dh5 cells were added to all the wellsexcept 1^{st} column wells which served as negative control.
7. The final volume in all the wells was 200ul.
8. The pre incubation reading was recorded with the help of 96 well platereader at 600nm.
9. The plate was incubated for 12h at 37 °C.
10. The post incubation reading was recorded after 12 h
11. The change in OD of each well was calculated by subtracting the initial OD(incubation = oh) from the final OD (incubation =12h)
12. OD around 0.0 indicated inhibition of growth of the indicator strain.

4.6 Precautions

- Zinc Nitrate Hexahydrate is highly hygroscopic in nature and hence must be made into solution form immediately after weighing, to avoid concentration aberrations.
- The final salt obtained through this Sol-Gel route is very less, of which scale-up is not possible due to the Sonication machine restriction. This process should therefore be repeated many times in order to obtain high amount of nanorods.
- Ethylenediamine is light sensitive, so reactions must be carried out under dark conditions only, the reaction volume must be covered with a black cloth at all times.
- Ethylenediamine, while stirring emits fumes which are highly oxidizing and can cause respiratory problems and bodily harm if in contact. Care must be taken to wear face mask and hand gloves while handling Ethylenediamine.

- While decanting the supernatant, some amount of salt is also lost. To minimize this, a dropper can be used to remove the supernatant without disturbing the cake of precipitate.
- The beakers and others equipments used should be washed carefully as presence of other materials may be disastrous for the reaction.
- Utmost care must be taken while handling the biological processes, as chances of contamination are very high. All exposure must be done under High Efficiency Particulate Air Filter Laminar hood only.

4.7 Characterization techniques

4.7.1 X-Ray Diffraction Analysis

X-ray powder diffraction (XRD) is a rapid analytical, non-destructive technique primarily used for phase identification of a crystalline material and can provide information on unit cell dimensions, chemical composition, and physical properties of materials. This technique is based on observing the scattered intensity of an X-ray beam hitting a sample as a function of incident and scattered angle, polarization, and wavelength or energy. Computer analysis of the peak positions and intensities associated with this pattern enables qualitative analysis, lattice constant determination and/or stress determination of the sample. Qualitative analysis may be conducted on the basis of peak height or peak area. The peak angles and profiles may be used to determine particle diameters and degree of crystallization, and are useful in conducting precise X-ray structural analysis. The identification of single or multiple phases in an unknown sample is the main application of X-ray powder diffractometry.

When a monochromatic X-ray beam with wavelength lambda is projected onto a crystalline material at an angle theta, diffraction occurs only when the distance traveled by the rays reflected from successive planes differs by a complete number n of wavelengths.

Bragg's Law

By varying the angle theta, the Bragg's Law conditions are satisfied by different d-spacings in polycrystalline materials. Plotting the angular positions and intensities of the resultant diffracted peaks of radiation produces a pattern, which is characteristic of the sample. Where a mixture of different phases is present, the resultant diffractogram is formed by addition of the individual patterns. The diffraction data is compared against a database maintained by International Centre for Diffraction Data.

X-ray diffractometers consist of three basic elements: an X-ray tube, a sample holder, and an X-ray detector. X-rays are generated in a cathode ray tube by heating a filament to produce electrons, accelerating the electrons toward a target by applying a voltage, and bombarding the target material with electrons. When electrons have sufficient energy to dislodge inner shell electrons of the target material, characteristic X-ray spectra are produced. These spectra consist of several components, the most common being K_α and K_β. K_α consists, in part, of $K_{\alpha 1}$ and $K_{\alpha 2}$.

Copper is the most common target material for single-crystal diffraction, with Cu K_α radiation = 0.5418Å. These X-rays are collimated and directed onto the sample. As the sample and detector are rotated, the intensity of the reflected X-rays is recorded. When the geometry of the incident X-rays impinging the sample satisfies the Bragg Equation, constructive interference occurs and a peak in intensity occurs. A detector records and processes this X-ray signal and converts the signal to a count rate which is then output to a device such as a printer or computer monitor. The geometry of an X-ray diffractometer is such that the sample rotates in the path of the collimated X-ray beam at an angle θ while the X-ray detector is mounted on an arm to collect the diffracted X-rays and rotates at an angle of 2θ. The instrument used to maintain the angle and rotate the sample is termed a *goniometer.*

4.7.2 FE-SEM Analysis

FESEM stands for Field emission scanning electron microscope. The FESEM is a microscope that uses electrons instead of light to form an image. Since their development in the early 1950's, scanning electron microscopes have developed new

areas of study in the medical and physical science communities. The FESEM has allowed researchers to examine a much bigger variety of specimens.

The scanning electron microscope has many advantages over traditional microscopes. The FESEM has a large depth of field, which allows more of a specimen to be in focus at one time. The FESEM also has much higher resolution, so closely spaced specimens can be magnified at much higher levels. Because the FESEM uses electromagnets rather than lenses, the researcher has much more control in the degree of magnification. All of these advantages, as well as the actual strikingly clear images, make the scanning electron microscope one of the most useful instruments in research today.

Various parts of FESEM: The sample is fixed with conductive tape on a metallic sample block. Non-conductive specimens are coated with a nanometer thin-layer of metal to facilitate emission and flow of electron in the surface. The metal block is crewed on a sample holder and positioned in the pre-vacuum chamber, an intermediate chamber with a front and a rear lid. This chamber acts as a lock. When the vacuum in this space is low enough the shutter to the high vacuum (lowest pressure) is opened and the object is shifted with a long rod into the object chamber on a rail just under the column. In order to ease the positioning a one can observe the inner view of the object chamber with an infra red camera. The object chamber is the place where the sample is irradiated by the electron beam. The position of the sample stage can be adjusted in height (z-navigation) and horizontally (x-y navigation). The topographical scanning electron imaging requires a secondary electrons detector; like in a normal SEM there is a control panel, a monitor for the operation of the device and one showing the SE images. A separate EDS detector allows one to capture the X-ray scanning and there is another back-scattered electron detector. In this chamber in the heart of the electron microscope the vacuum is extremely low: 10^{-6}mBar (thus 1:1.000.000.000 the normal atmospheric pressure; vacuum display = 16; around the electron gun the vacuum is even two orders of magnitude lower). The need for such extreme vacuum is that collision of bombarding electrons from the beam with gas molecules in the column would result in heat production. Cooling and supply of electric power are required in order to maintain this extreme vacuum.

Under vacuum, electrons generated by a Field Emission Source are accelerated in a field gradient. The beam passes through Electromagnetic Lenses, focussing onto the specimen. As result of this bombardment different types of electrons are emitted from the specimen. A detector catches the secondary electrons and an image of the sample surface is constructed by comparing the intensity of these secondary electrons to the scanning primary electron beam. Finally the image is displayed on a monitor.

In SEM the image is formed from secondary electrons that have been dislocated at the surface of the scanned sample by bombarding primary electrons from the electron gun. Those ejected electrons are captured by a detector and the information is converted into an electric signal, amplified and digitalized. The result is a topographical image of the surface of the object, e.g. the surface of a metal coating or lamellae of fish gills (see example here below). Besides secondary electrons, radiation (in particular X-rays and cathodoluminescence in typical samples) as well as back-scattered and so-called Auger electrons with an own energy level are produced upon interaction of atoms in the surface layer of the sample with the primary electron beam. These emission signals, which contain information among others on the element composition of the upper layer, can be received by selected detectors, as is the case in EDAX microscopes for example, and combined with the topographical image.

Besides, there are scanning electron microscopes which are equipped with EDS (Energy Dispersed Spectroscopy) or EDAX (Energy-Dispersed Analysis of X-rays) detectors that capture the emitted X-ray. With such instruments it is possible to determine *which elements* are present in the surface layer of the sample (at a depth in the micrometer range) and *where* these elements are present ("mapping technique"). This particular microscope also allows one to capture directly reflected electrons, the so-called back scattered electrons, from which one can obtain a global appreciation whether one or several elements are present in the surface layer of the sample. Also the so-called Auger electrons, which are emitted just under the surface, provide information about the nature of the atoms in the sample.

SAMPLE PREPARATION FOR FESEM: Because the SEM utilizes vacuum conditions and uses electrons to form an image, special preparations must be done to the sample. All water must be removed from the samples because the water would vaporize in the vacuum. All metals are conductive and require no preparation before being used. All non-metals need to be made conductive by covering the sample with a thin layer of conductive material. This is done by using a device called a "sputter coater."

The sputter coater uses an electric field and argon gas. The sample is placed in a small chamber that is at a vacuum. Argon gas and an electric field cause an electron to be removed from the argon, making the atoms positively charged. The argon ions then become attracted to a negatively charged gold foil. The argon ions knock gold atoms from the surface of the gold foil. These gold atoms fall and settle onto the surface of the sample producing a thin gold coating.

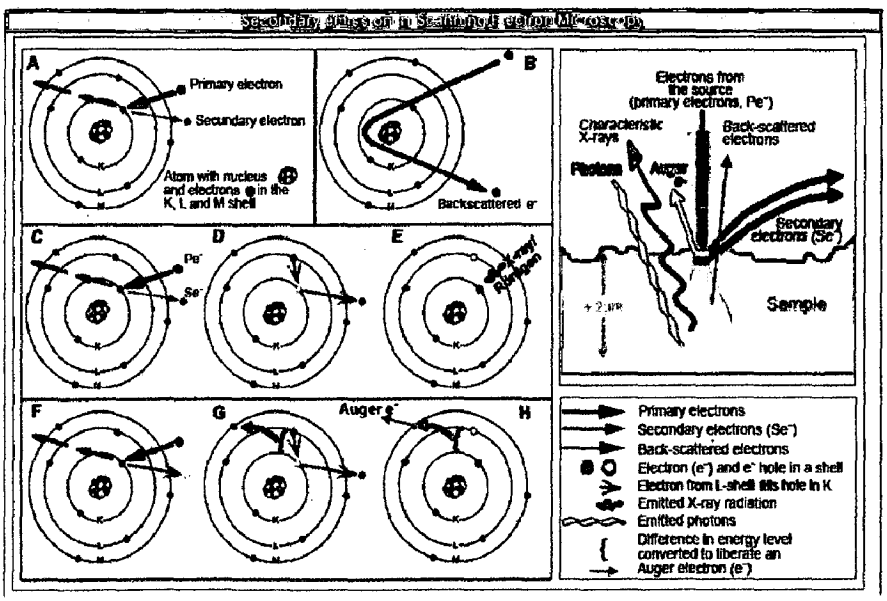

Fig. 4.2: Emissions in SEM

A: The bombarding electrons (=primary electrons) can penetrate in the electron shells of the atoms composing the surface of the sample. The energy (negative charge, mass, velocity) of these incident electrons can be converted to eject local electrons, so-called secondary electrons, from the shells of the atoms in the surface of the specimen. This information cab ne utilized to reconstruct a detailed topographical image of the sample (SEI = Secondary Electrons Imaging). The final image looks like a shadow-

cast photograph of the surface of the sample. This record of the morphology is the best-known application of a scanning electron microscope.

B: Primary electron can also be reflected by atoms at about 10-100 nanometre depth at the surface. These so-called "back-scatter" conserve their energy at incidence, but their direction of propagation has been modified upon interaction. One can obtain a rough representation whether the surface of the sample is constituted of a single or multiple elements.

C, D, E: at the surface of the sample electrons in the deeper electron shells (shell K in **C**) can be ejected by primary electrons (Pe-indicated in red), resulting in an electron hole. When this lower-shell position is filled by an electron from higher shell (green arrow in **D**) energy is released. This can be as light (photons; the phenomenon is also called cathode luminescence) or as X-ray. Because each element emits an own characteristic energy value, the elements present in the micrometer range depth of the sample can be determined. See example here below.

F, G, H: another phenomenon is that the energy released upon filling a hole in the K shell by an electron from the L shell is used to expulse an electron from the external M shell: a so-called Auger electron. The released energy is characteristic for the type of atom. Auger electrons are produced in the outermost surface layer (at nanometer depth) of the sample.

4.7.3 EDAX Analysis

Energy dispersive X-ray spectroscopy (EDS) is an analytical technique used for the elemental analysis or chemical characterization of a sample. It is one of the variants of XRF. As a type of spectroscopy, it relies on the investigation of a sample through interactions between electromagnetic radiation and matter, analyzing x-rays emitted by the matter in response to being hit with charged particles. Its characterization capabilities are due in large part to the fundamental principle that each element has a unique atomic structure allowing x-rays that are characteristic of an element's atomic structure to be identified uniquely from each other.

To stimulate the emission of characteristic X-rays from a specimen, a high energy beam of charged particles such as electrons or protons, or a beam of X-rays, is focused into the sample being studied. At rest, an atom within the sample contains ground state (or unexcited) electrons in discrete energy levels or electron shells bound to the nucleus. The incident beam may excite an electron in an inner shell, ejecting it from the shell while creating an electron hole where the electron was. An electron from an outer, higher-energy shell then fills the hole, and the difference in energy between the higher-energy shell and the lower energy shell may be released in the form of an X-ray. The number and energy of the X-rays emitted from a specimen can be measured by an energy dispersive spectrometer. As the energy of the X-rays is characteristic of the difference in energy between the two shells, and of the atomic structure of the element from which they were emitted, this allows the elemental composition of the specimen to be measured.

4.7.4 MIC Assay machine (96 Well Plate Reader)

The 96 well plate reader is a high throughput and efficient measurement device meant for reading optical density of the samples. The basic principle underlying the mechanism is the Beer-Lambert Law. The Beer-Lambert law (or Beer's law) is the linear relationship between absorbance and concentration of an absorbing species. The general Beer-Lambert law is usually written as:

$$A = a\ (lambda) * b * c$$

Where A is the measured absorbance, a(lambda) is a wavelength-dependent absorptivity coefficient, b is the path length, and c is the analyte concentration. When working in concentration units of molarity, the Beer-Lambert law is written as:

$$A = epsilon * b * c$$

Where epsilon is the wavelength-dependent molar absorptivity coefficient with units of $M^{-1}\ cm^{-1}$.

Experimental measurements are usually made in terms of transmittance (T), which is defined as:

$$T = I / I_o$$

Where I is the light intensity after it passes through the sample and Io is the initial light intensity. The relation between A and T is:

$$A = -\log T = -\log (I / I_o).$$

Absorption of light by a sample:

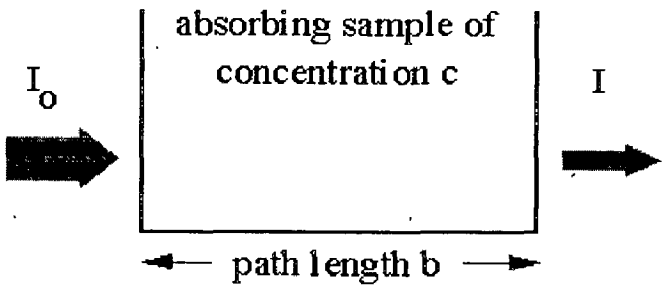

Fig 4.3: Pictorial representation of the Beer-Lambert's Law.

Modern absorption instruments can usually display the data as transmittance, %-transmittance, or absorbance. An unknown concentration of an analyte can be determined by measuring the amount of light that a sample absorbs and applying Beer's law. If the absorptivity coefficient is not known, the unknown concentration can be determined using a working curve of absorbance versus concentration derived from standards.

Limitations of the Beer-Lambert law:

The linearity of the Beer-Lambert law is limited by chemical and instrumental factors. Causes of nonlinearity include:

- deviations in absorptivity coefficients at high concentrations (>0.01M) due to electrostatic interactions between molecules in close proximity
- scattering of light due to particulates in the sample
- fluoresecence or phosphorescence of the sample

- changes in refractive index at high analyte concentration
- shifts in chemical equilibria as a function of concentration
- non-monochromatic radiation, deviations can be minimized by using a relatively flat part of the absorption spectrum such as the maximum of an absorption band
- stray light

CHAPTER 5

RESULTS AND DISCUSSIONS

5.1 Synthesis of Nanorods:

The Sol-Gel method employed here for synthesis of nanorods is successful only when a capping agent is used.

5.1.1 With Ethylenediamine as capping agent

Initially, the reaction is optimized with and without capping agents. Figures 5.1, 5.2, 5.3, 5.4 and 5.5 are FESEM micrographs of product in the presence of capping agent. The zinc hydroxide was first calcinated at 150°C for 5 hours, and then washed thrice with water and once with methanol.

Figures 5.6, 5.7, are FESEM micrographs of product synthesized without any capping agent.

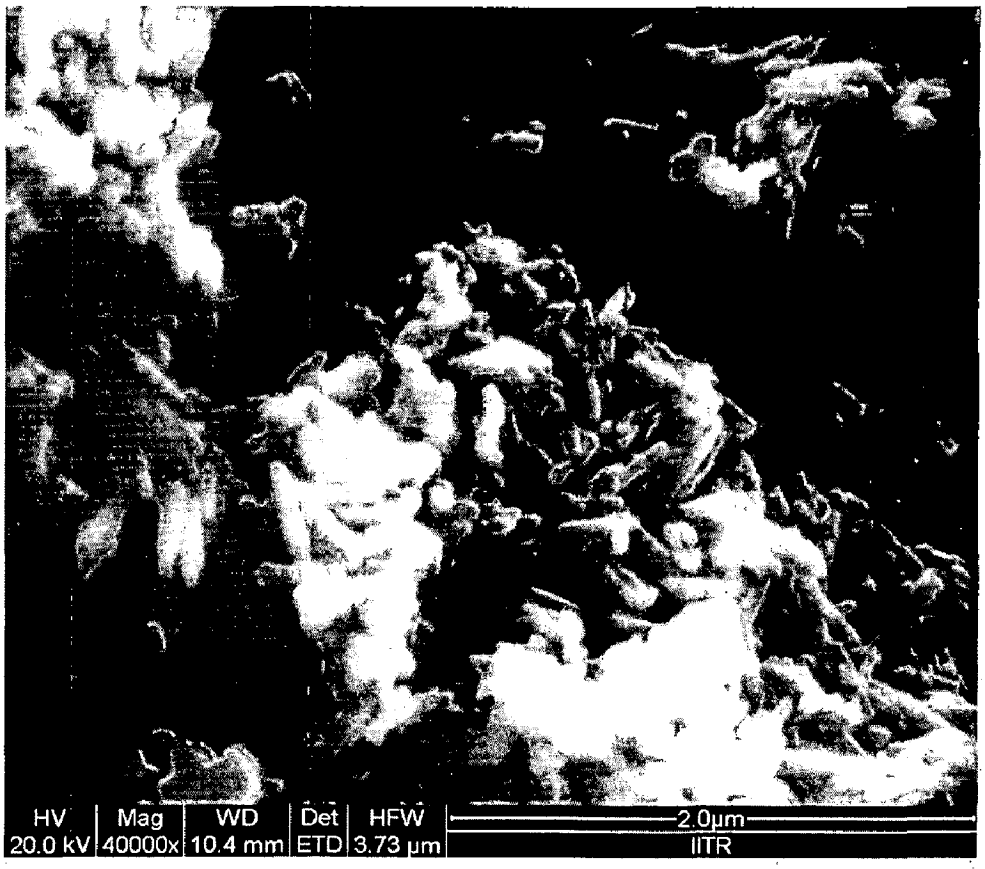

Figure 5.1: FESEM micrograph at 40000x of product synthesized using EDA as capping agent

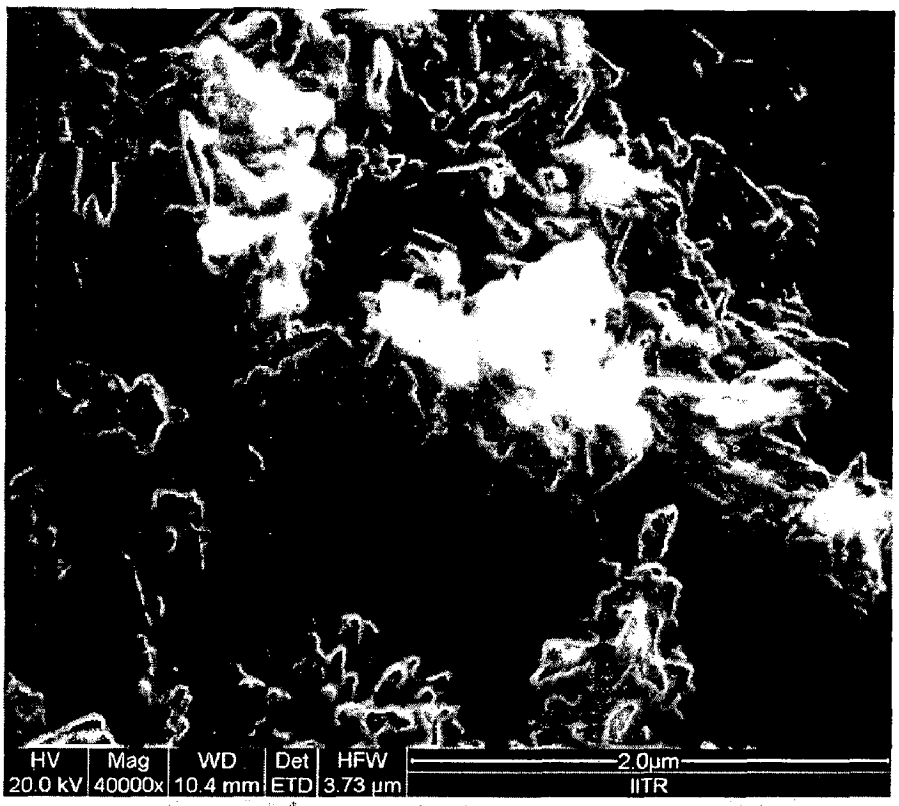

(5.2)

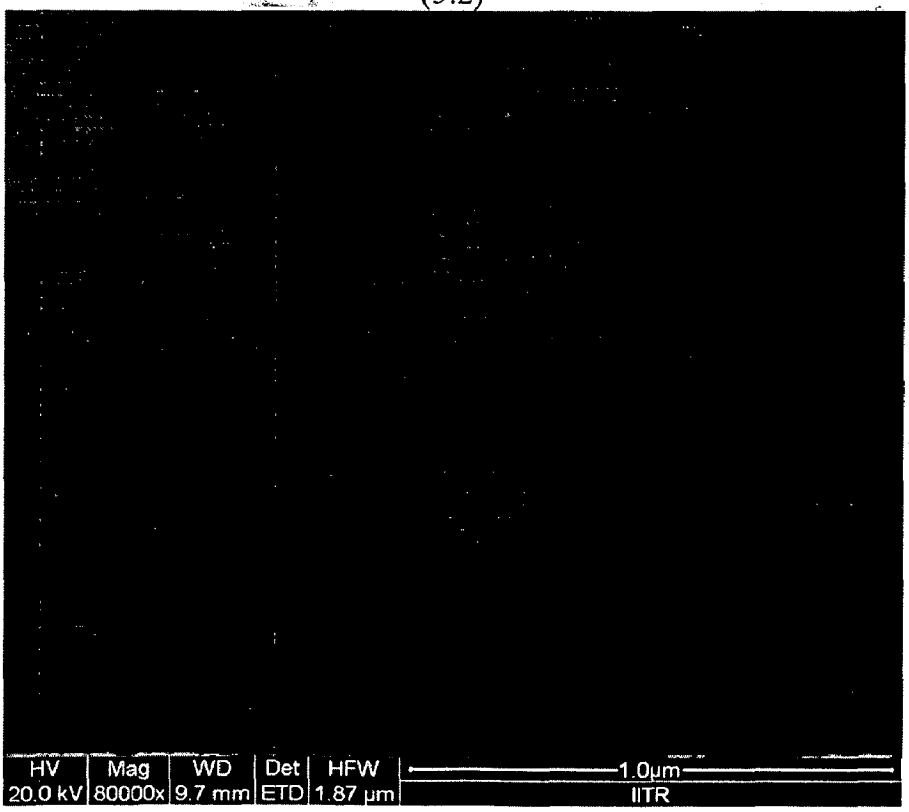

(5.3)

Figure: FESEM micrographs of nanorods at (5.2) 40000x and at (5.3) 80000x

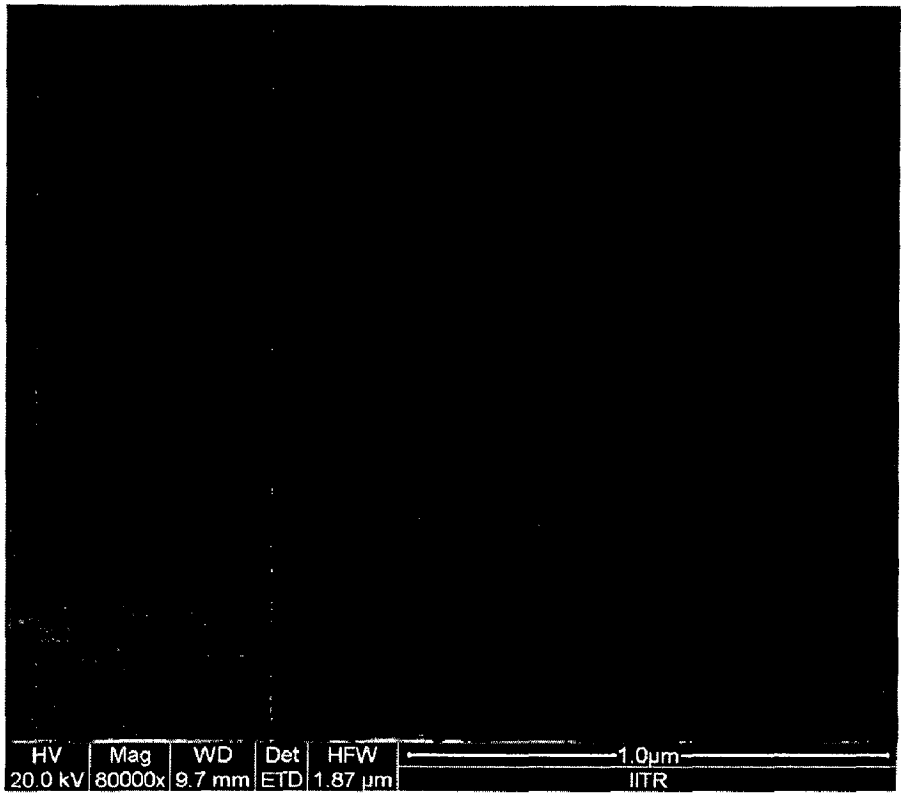

(5.4)

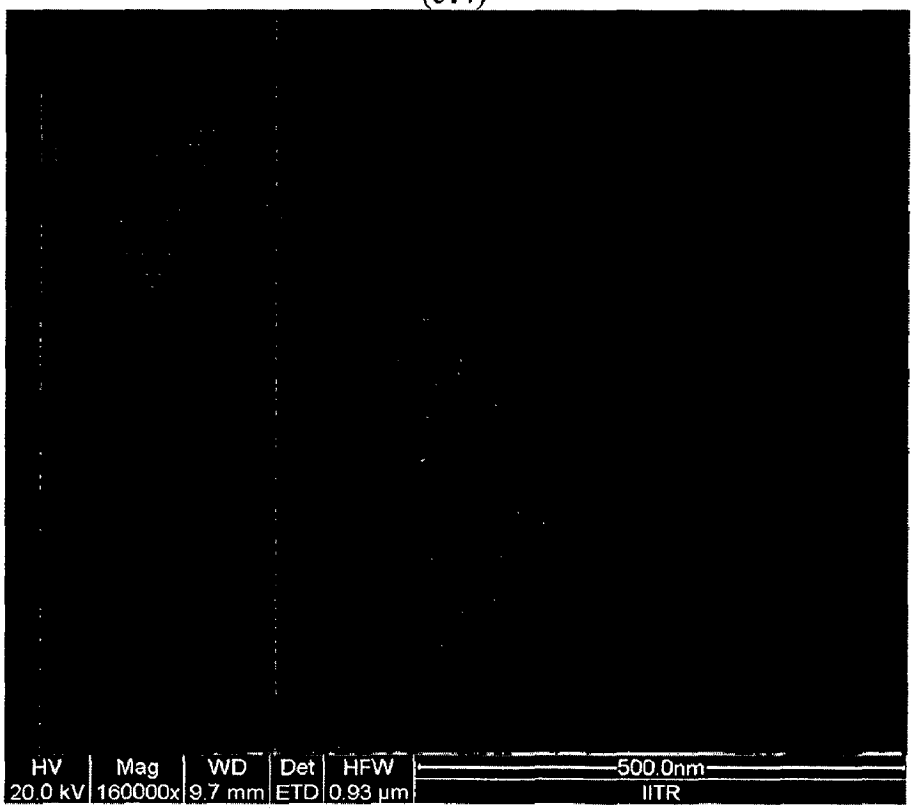

(5.5)

Figure: FESEM micrographs of nanorods at (5.4) 80000x and at (5.5) 160000x

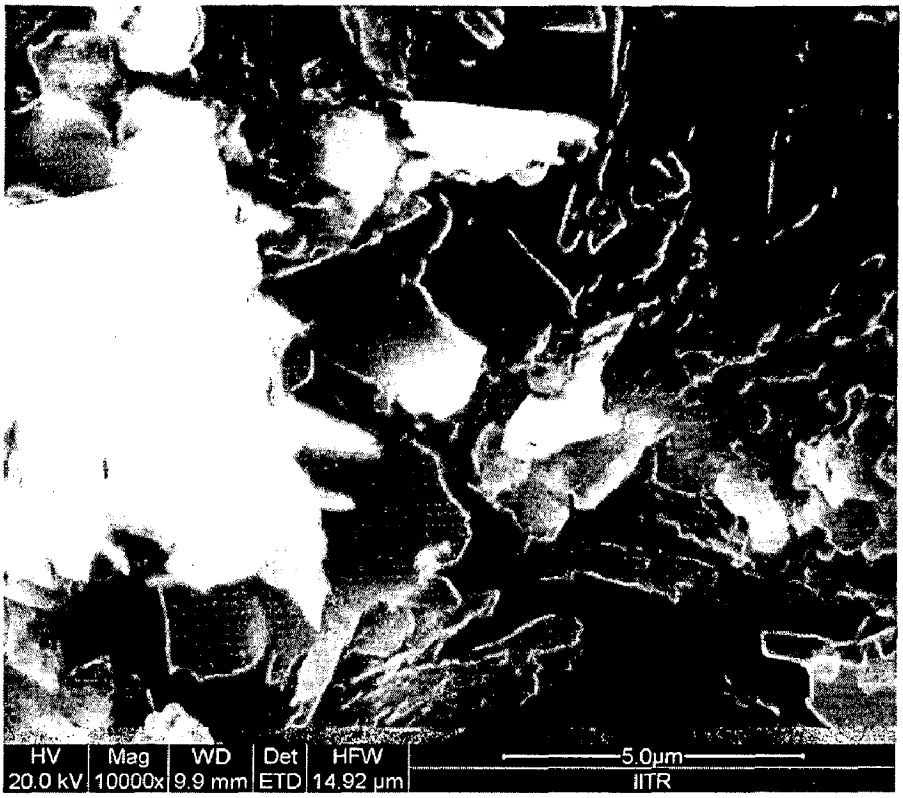

(5.6)

(5.7

Figures 5.6 and 5.7: FESEM micrographs of product synthesized without capping agent

It now becomes evident from the FESEM micrographs that capping agent not only serves as an inhibitor in fusion of the Nanosized ZnO, but also to restrict the growth of the nanorods after a certain length. In this case the length of the nanorods can be gauged from the micrograph as approximately **300nm**.

And, the Aspect Ratio is calculated as: A.R = Length (nm) / Breadth (nm)

Therefore, **A.R.** = 300nm / 80 nm = **3.75**

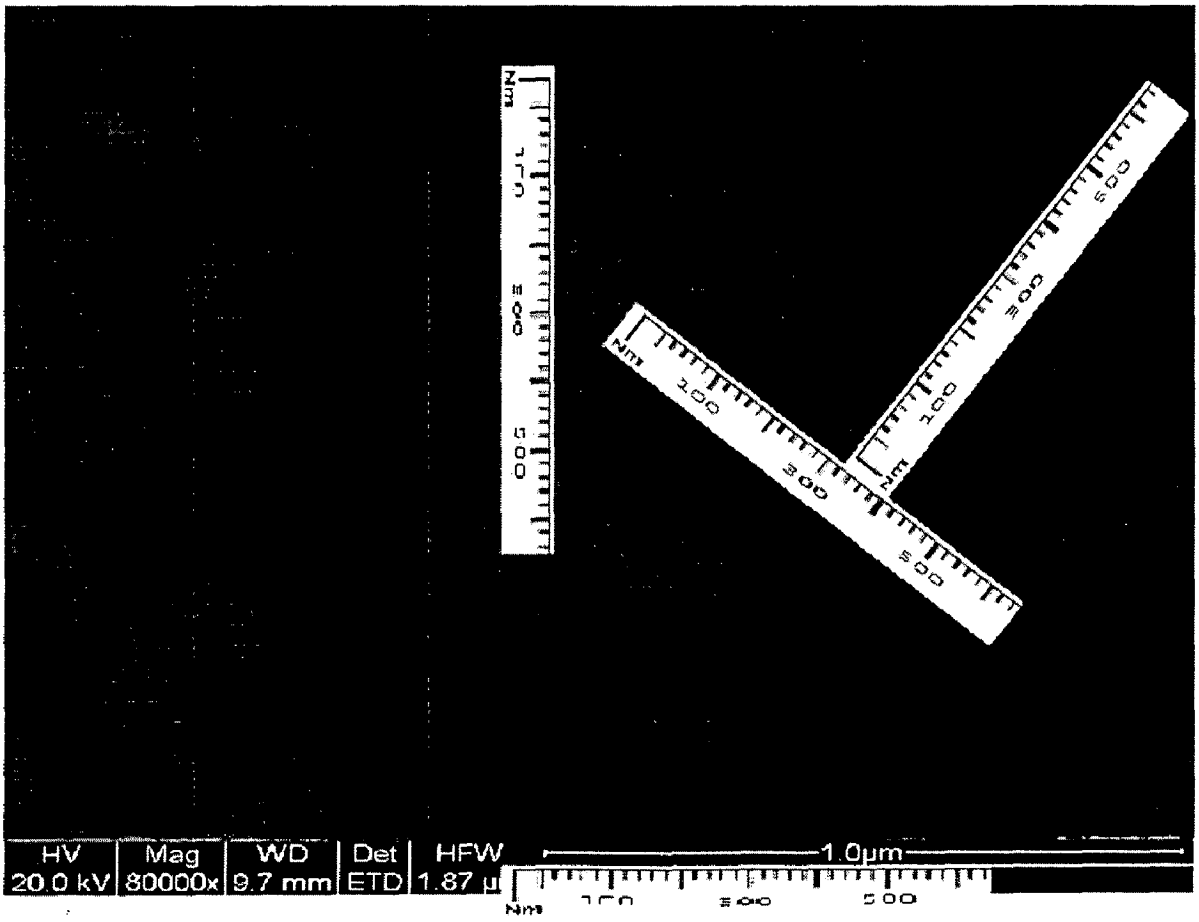

Figure 5.8 FESEM micrograph showing approximate size of synthesized nanorods

5.1.2 E-DAX analysis

The E-DAX analysis of this product indicates that the Zinc Hydroxide has been efficiently oxidized, as a result of which Zinc Oxide nanorods are formed. Any left over Zinc Hydroxide is separated by washing with water, as Zinc Hydroxide is soluble in water and Zinc Oxide is not soluble. Given below is the E-DAX of Figure 5.4

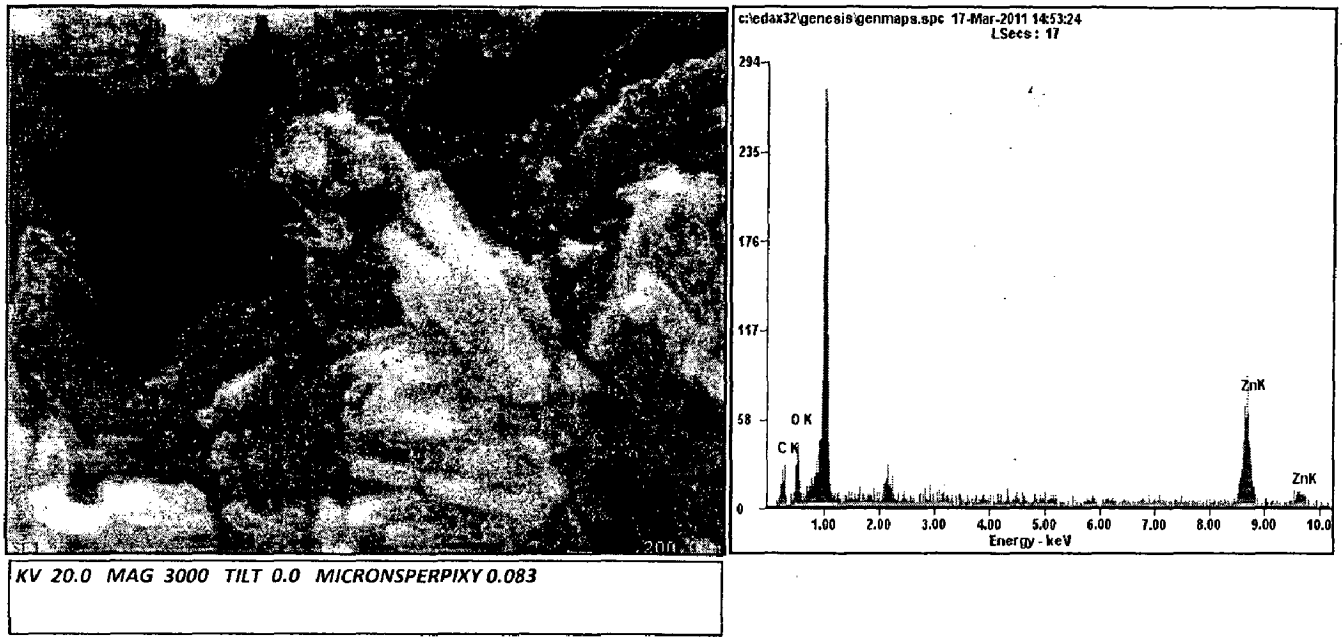

Figure 5.4 (a): FESEM micrograph of ZnO synthesized by using Ethylenediamine as capping agent, and graph showing composition of elements.

Element	*Wt%*	*At%*
CK	25.28	56.79
OK	09.72	16.38
ZnK	65.00	26.83
Matrix	Correction	ZAF

Table 1: E-DAX analysis of ZnO nanorods synthesized using Ethylenediamine as capping agent.

5.2 With Citric Acid Monohydrate as capping agent

In the same way, when a negatively charged compound such as **Citric Acid Monohydrate** is used as a **capping agent**, ZnO nanorods are formed. However, the final product not only contains nanorods but also nanostructures with various morphologies.

5.2.1 With Citric Acid Monohydrate as capping agent, calcinated at 170°C

By varying the temperature for calcinations, a certain degree of control can be obtained and the process can be fine tuned to produce near perfect nanorods or nanospheres. Figures 5.9 and 5.10 show FESEM micrographs of product which is calcinated at 170°C for 12 hours.

Figure 5.9 FESEM micrograph of ZnO synthesized by using Citric Acid Monohydrate as capping agent.

The approximate size of Zn nanorods synthesized with Citric Acid Monohydrate as capping agent is **250 nm to 350nm.** From the Figure 5.10, the approximate Aspect Ratio can be measured as **A.R** = 300nm / 60nm = **5**

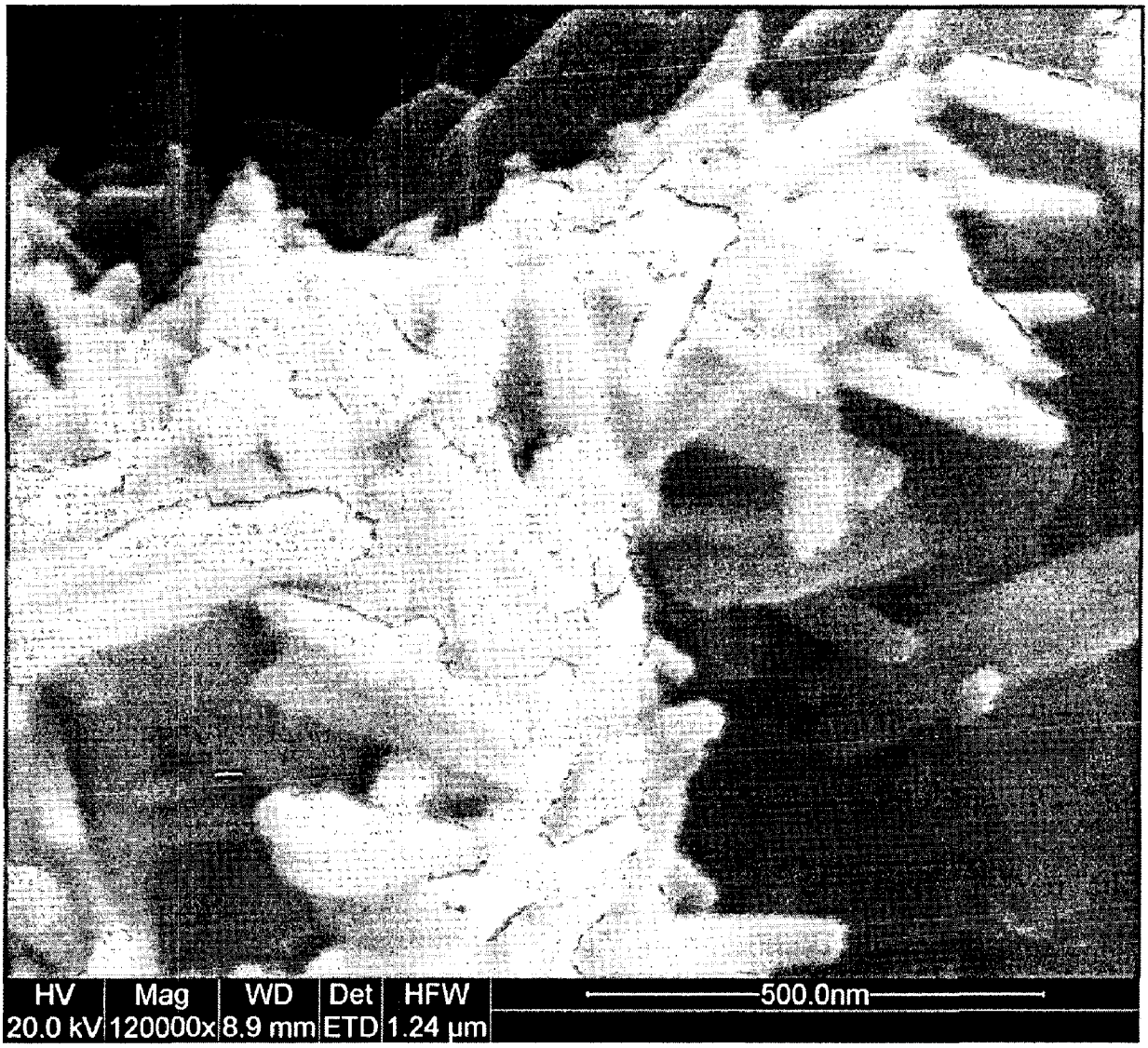

Figure 5.10 FESEM micrograph of ZnO synthesized by using Citric Acid Monohydrate as capping agent showing the dimensions of the nanorods

5.2.1.1 EDAX analysis

EDAX analysis of the ZnO nanorods synthesized by using Citric Acid Monohydrate shows that the Sodium ions are bound tightly to the compound and is not removed even after washing repeatedly with water. Given below is the E-DAX of Figure 5.10.

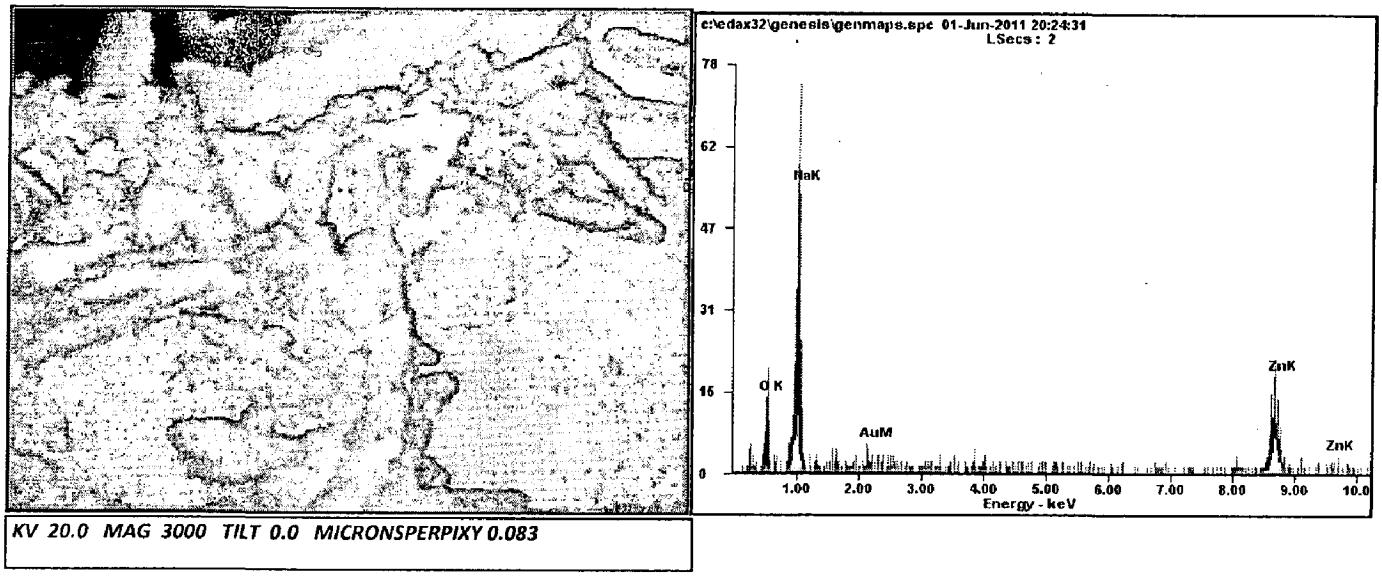

Figure 5.10 (a): FESEM micrograph of ZnO synthesized by using Citric Acid Monohydrate as capping agent, and graph showing composition of elements.

Element	Wt%	At%
OK	08.24	17.00
NaK	41.41	59.46
AuM	05.60	00.94
ZnK	44.76	22.60
Matrix	Correction	ZAF

Table 2: E-DAX analysis of ZnO nanorods synthesized using Citric Acid Monohydrate as capping agent.

5.2.2 With Citric Acid Monohydrate as capping agent, calcinated at 150°C

When the same process was employed and the product was calcinated at 150°C for 12 hours, the formation of nanorods is minimized and no other clear shape is observed. Figure 5.11 shows the FESEM micrograph of product showing mixture of nanorods and other mosaic agglomerates.

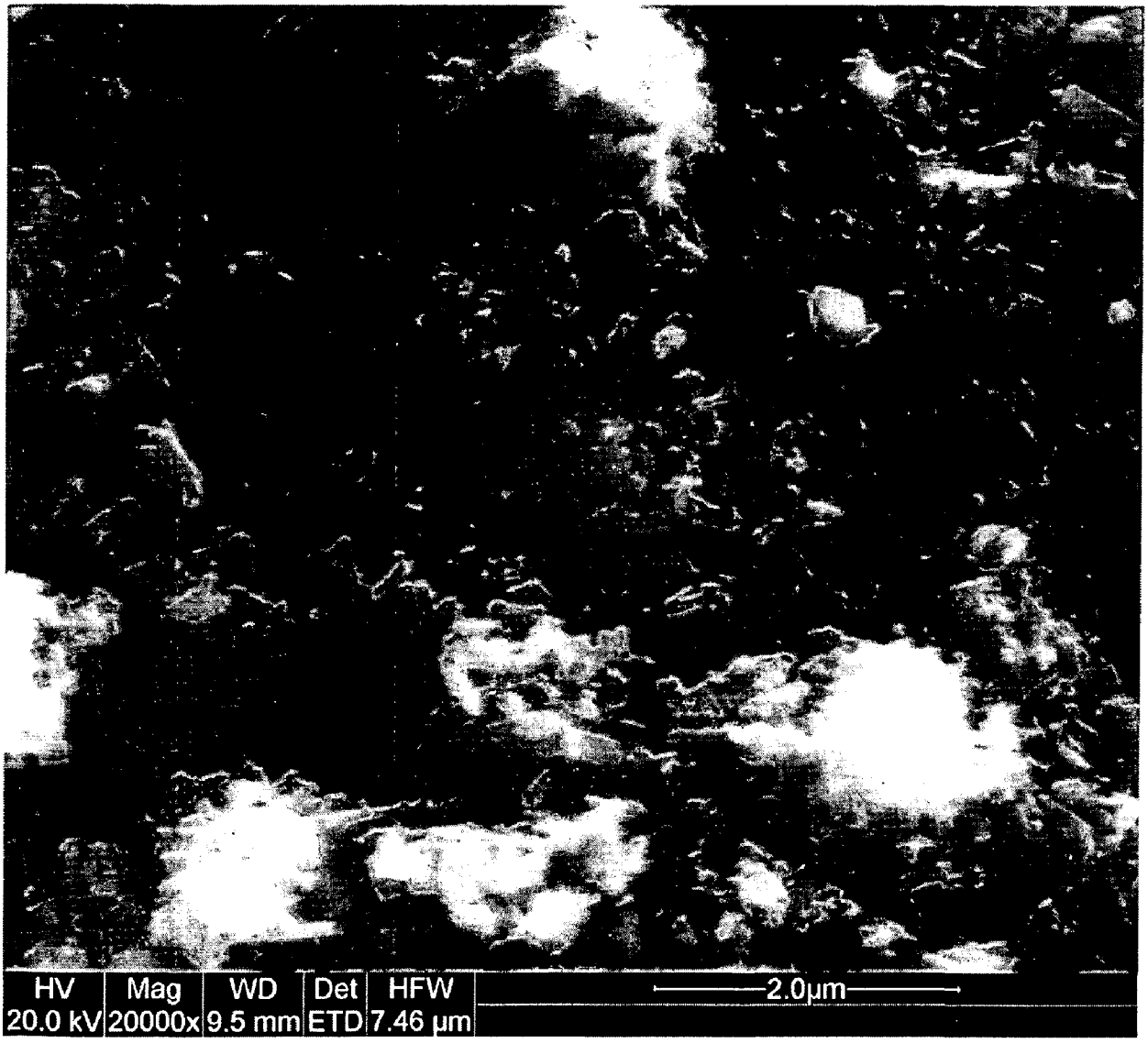

Figure 5.11 FESEM micrograph of ZnO synthesized by using Citric Acid Monohydrate as capping agent and calcinated at 150°C for 12 hours.

5.2.3 With Citric Acid Monohydrate as capping agent, calcinated at 125°C

Finally, when calcination is carried out at **125°C**, the formation of nanorods is completely stopped, instead, agglomerates of **nanospheres** are observed. Figure 5.12 show FESEM micrograph of product synthesized by using Citric Acid Monohydrate as capping agent calcinated at 125°C for 12 hours.

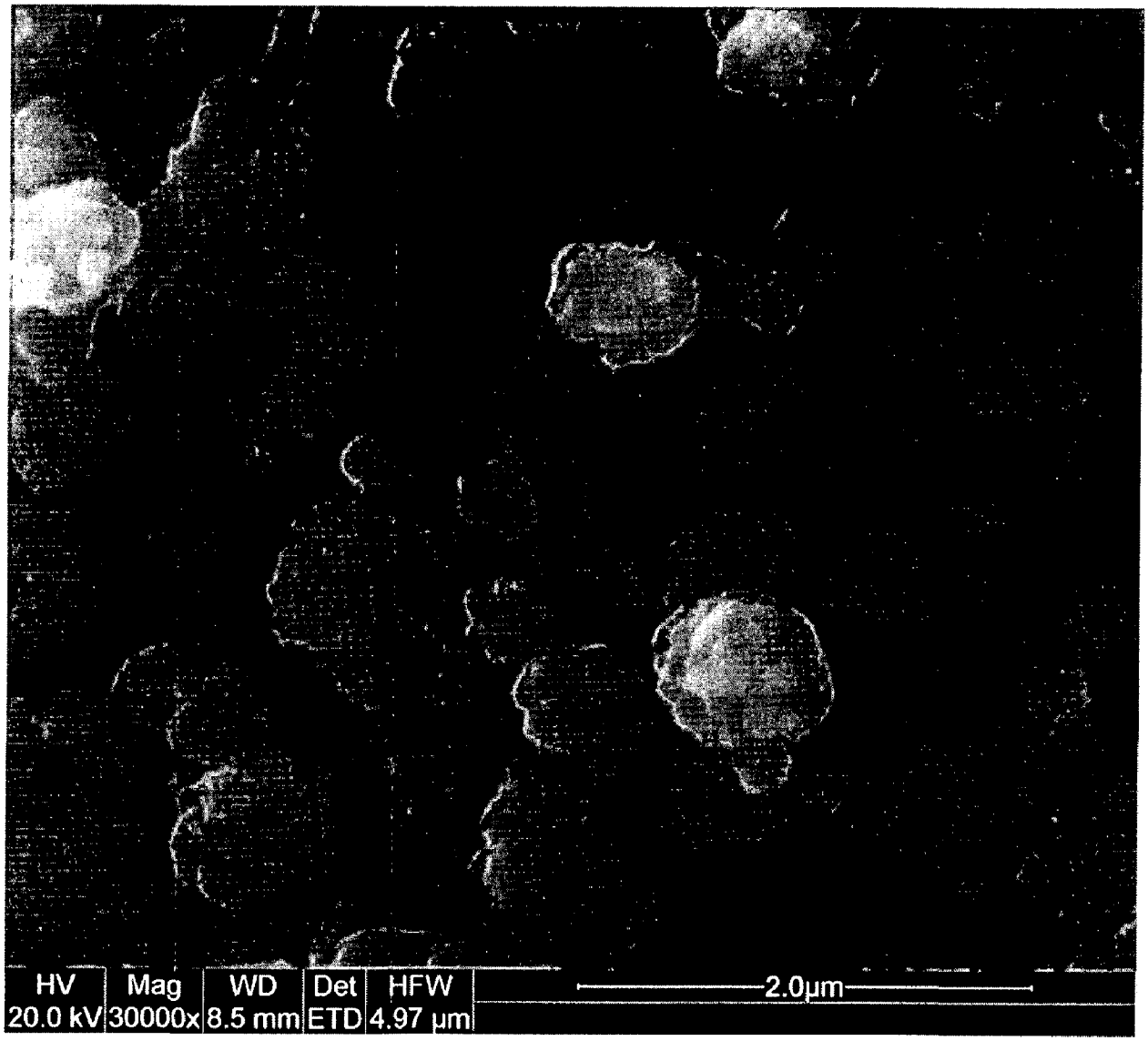

Figure 5.12 (a): FESEM micrograph of ZnO synthesized by using Citric Acid Monohydrate as capping agent and calcinated at 125°C for 12 hours.

From Figure 5.12 (b), the size of such Nanospheres can be determined as 200nm (dia) and the size of the agglomerates of the nanospheres can be determined as 800nm (dia) approximately.

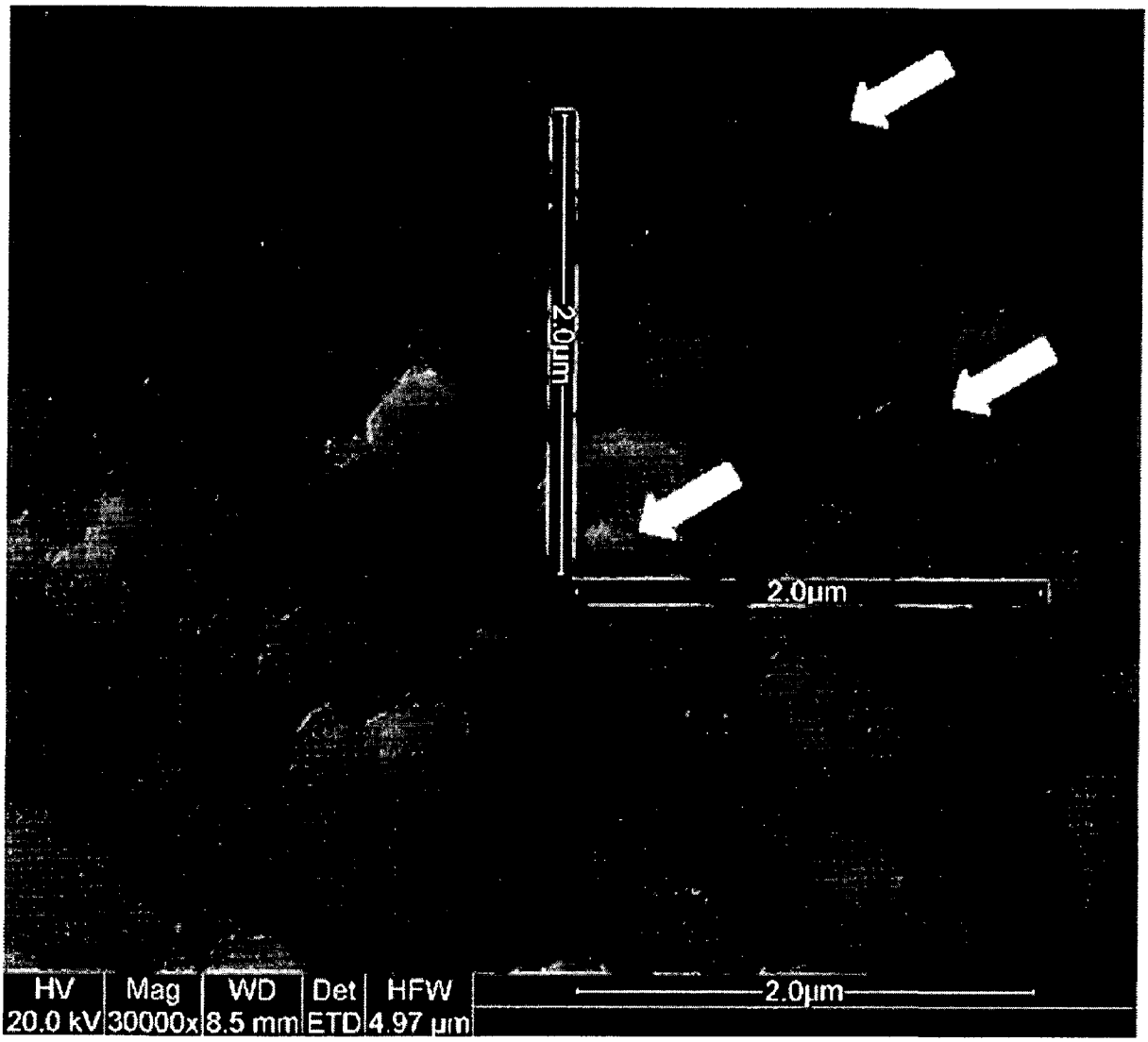

Figure 5.12 (b): FESEM micrograph of ZnO synthesized by using Citric Acid Monohydrate as capping agent and calcinated at 125°C. The arrows point out the individual nanospheres and agglomerates of nanospheres.

5.3 Anti-Microbial Activity

5.3.1 Qualitative tests (Preliminary)

ZnO nanorods synthesized by using Ethylenediamine as capping agent were tested against Gram Negative E. coli ATCC 25922 and against Gram Positive *Micrococcus leuteus* bacterium to evaluate its antibacterial potential. Initially we have tested a number of compounds using spot on lawn assay to determine qualitative antibacterial activity.

A clear zone of inhibition was observed against E. coli ATCC 25922 with pre-washed nanorods that were calcinated at 150°C. On the other hand there was no such zone observed in other samples (fig. s). Interestingly no activity is observed when the same samples tested against Gram Positive *Micrococcus leuteus* as evident from Figure 5.14.

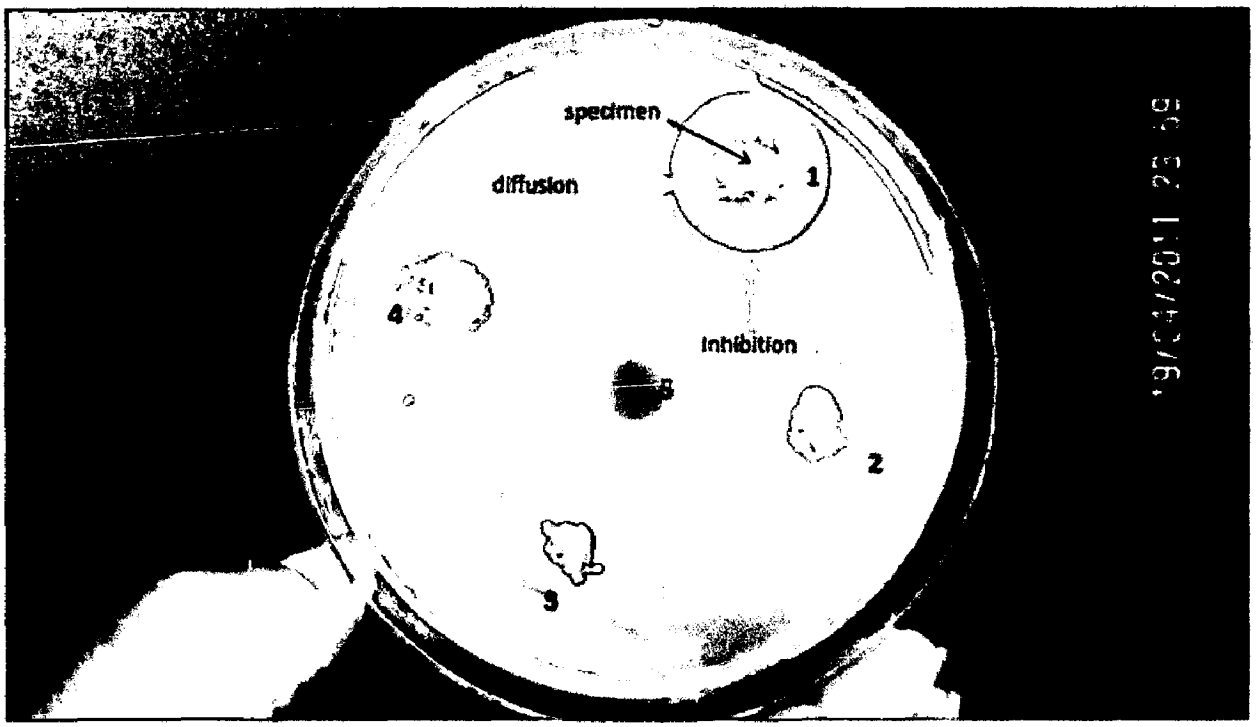

Figure 5.13: Spot-on-Lawn test, depicting the activity of ZnO nanorods against ***E.Coli*** **ATCC 25922** strain. Here: 1 - pre-washed and calcinated at 120°C, 2-calcinated at 120°C and washed, 3-calcinated at 140°C and washed, 4-calcinated at 160°C and washed, 5- supernatant from washing.

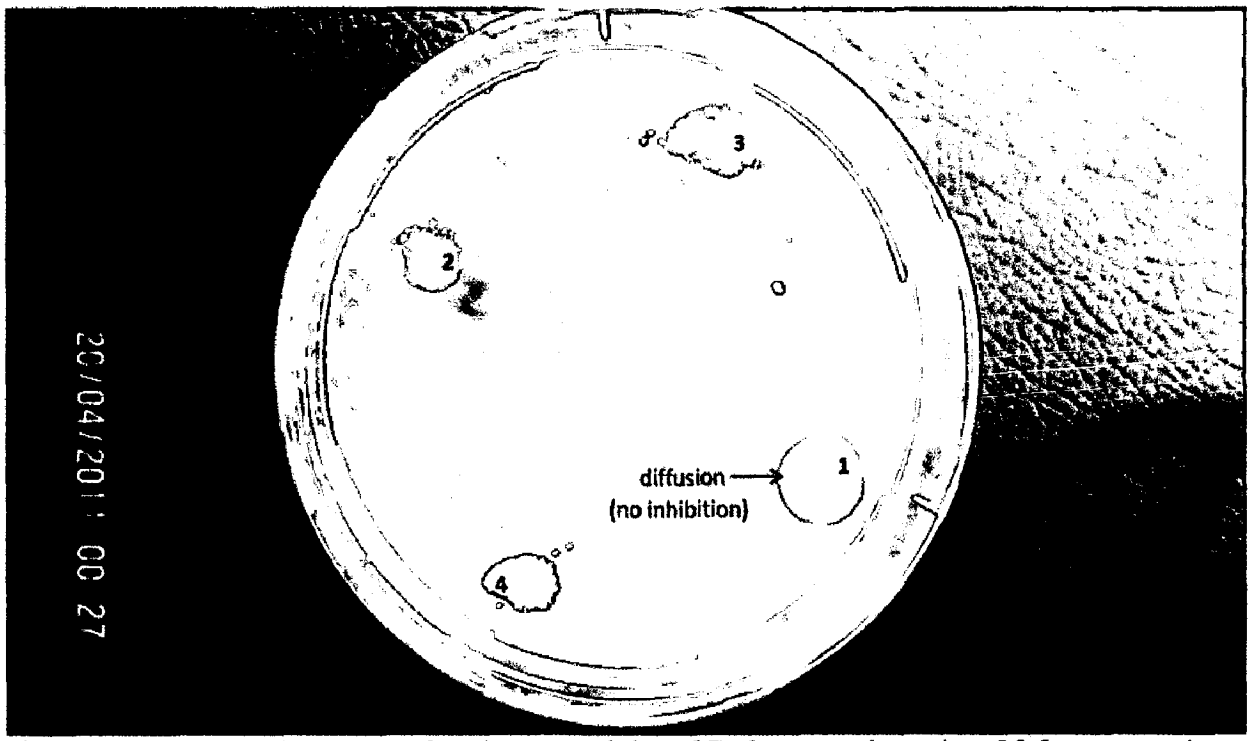

Figure 5.14: Spot-on-Lawn test, showing no activity of ZnO nanorods against ***M. leuteus*** strain. Here: 1 - prewashed and calcinated at 120°C; 2, 3, and 4 - calcinated at 120°C, 140°C, 160°C and washed respectively.

Further, ZnO nanorods synthesized via Sol-Gel method by using **Citric Acid Monohydrate** as **capping agent** were tested against Gram Negative *E.Coli* ATCC 25922 strain and against Gram Positive *Bacillus subtilis.* After 36 hours, no activity was observed against Gram negative *E. Coli* ATCC 25922 strain (Figure 5.15) while a distinct zone of inhibition was observed against Gram Positive B. Subtilis (Figure 5.16). Diffusion of pre-washed sample (prior to calcination) (sample No.1 in Figure 5.15) occurred in the LB Agar medium, but when nanosized ZnO was washed after calcination, diffusion does not occur. (Sample No. 2, 3 and 4)

The ZnO nanorods showed comparatively lesser diffusion when tested against **B. Subtilis** but still, a clear **zone of inhibition** is observed (Figure 5.16).

The dry powder of ZnO nanorods which showed bactericidal activity in the preliminary tests were further tested for quantification of anti-bacterial activity.

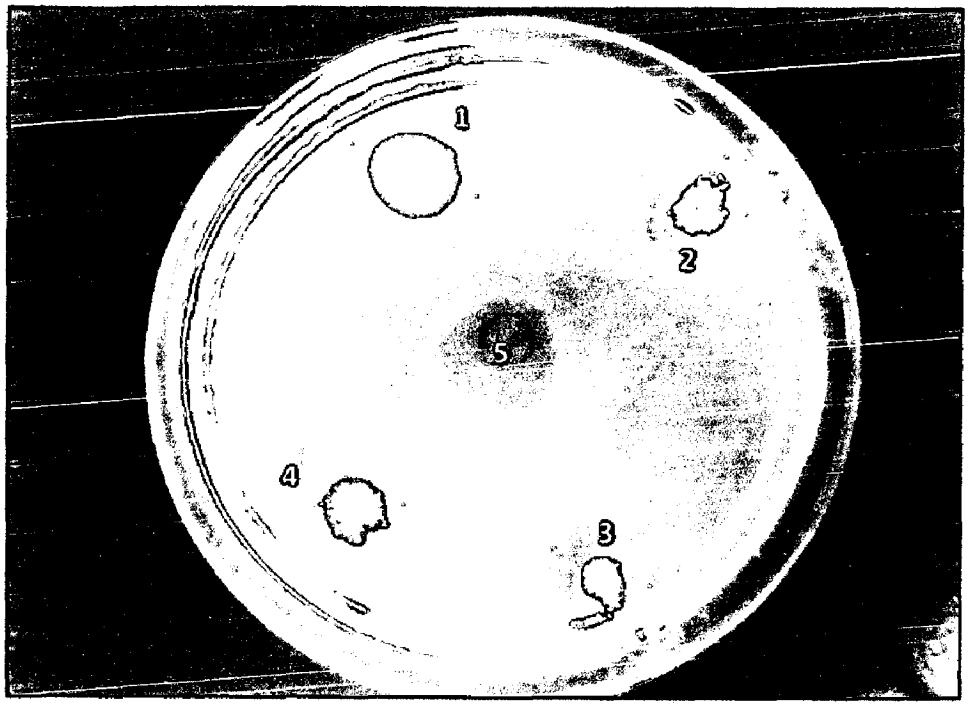

Figure 5.15: Spot-on-Lawn test, showing **no activity** of ZnO nanorods (with CAM as capping agent) against **E. coli** strain. Here: 1 - prewashed and calcinated at 120°C; 2, 3, and 4 - calcinated at 120°C, 140°C, 160°C and washed respectively.

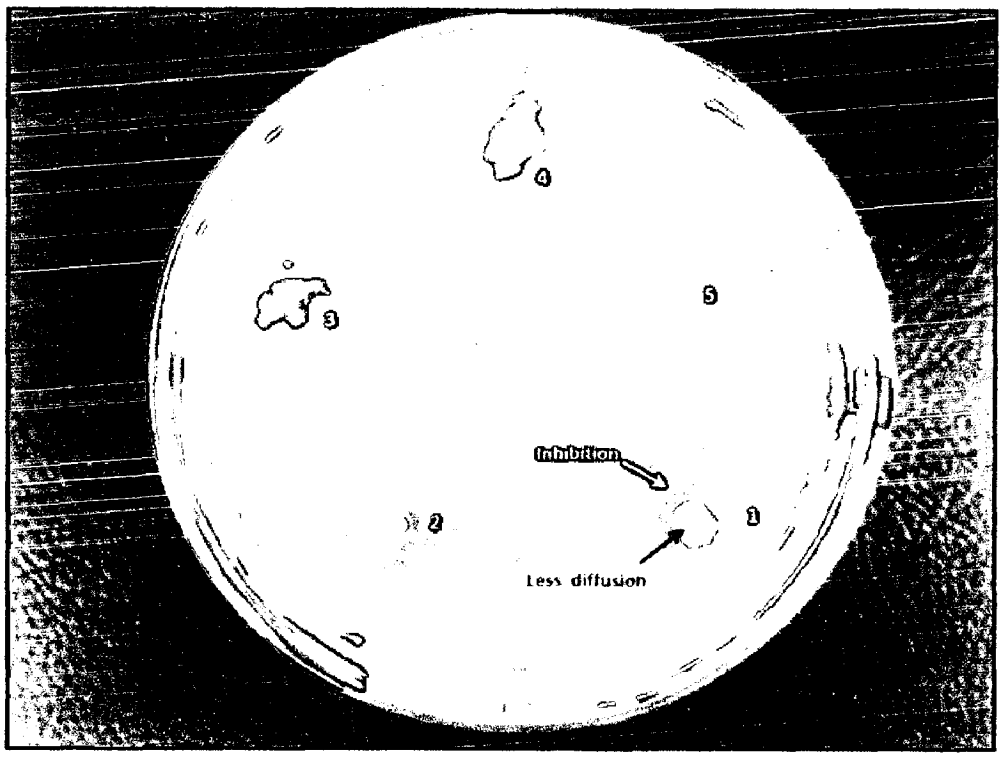

Figure 5.16: Spot-on-Lawn test, depicting the activity of ZnO nanorods against **B. subtilis**. Here: 1-calcinated at 120°C and washed, 2 - pre-washed and calcinated at 120°C, 3-calcinated at 140°C and washed, 4-calcinated at 160°C and washed, 5-calcinated at 180°C and washed.

5.3.2 Determination of minimum inhibitory concentration (MIC) of ZnO rods against bacterial pathogens (quantitative test):

MIC Assay of ZnO was carried out. 4 variants of ZnO nanorods were tested.

The minimum inhibitory concentration against *E.Coli* ATCC 25922 was sought for the following:

1. Methanol
2. ZnO nanorods suspended in water.
3. ZnO nanorods suspended in methanol

Known quantity of the nanorods synthesized with Ethylenediamine as capping agent was suspended in methanol and pure water separately, and was serially diluted in the 96 well plates. Measurements of Optical Density pre-incubation and post-incubation -after allowing 24 hours of incubation time at room temperature – are read. The difference between the measurements of Optical Density of the pre read data and the post read data is analyzed.

The least amount of antibacterial agent required to prevent the growth of the bacteria is designated as the Minimum Inhibitory Concentration. Table 3 gives the MIC of the ZnO nanorods against E. coli.

The minimum inhibitory concentration for **E. coli ATCC 25922** is found to be:

Sl.No	Antibacterial Agent	Minimum Inhibitory Concentration (MIC) for E. coli ATCC 25922
1	Pure Methanol	**1.33** mg/ml
2	ZnO dissolved in Methanol	**0.332** mg/ml
3	ZnO dissolved in Water	**1.33** mg/ml

Table 3: Values of MIC against *E.Coli* ATCC 25922 obtained from 96 well plate reader.

The synergistic bactericidal activity of Methanol as well as Zinc Oxide nanorods is corroborated by the reduction in the value of MIC for ZnO suspended in Methanol.

The mechanism of bacteria inactivation by ZnO Nanoparticles has been suggested as particle-induced reactive-oxygen-species (ROS) production and oxidative injury inside

bacterial cells by Applerot *et al.* [51] Additional mechanisms like membrane dysfunction, and nanoparticle internalization [14] have also been reported.

Here, the selective toxicity of a positively charged capping agent (Ethylenediamine) towards Gram negative *E.Coli* ATCC 25922 hypothesis that the capping agent facilitates in binding and/or attachment of the nanorods to the surface of bacterium. Inhibition of Gram negative bacteria by nanorods prepared in the presence of a negatively charged capping agent (Citric Acid Monohydrate) is considered as the positive capping agent facilitating the attachment of toxic nanorods to peptidoglycan chains of the bacterial cell surface. The mechanism of action could be in isolation or combination of any of the three causes mentioned above.

CONCLUSIONS

The following conclusions were drawn after performing and observing the experimental work in this thesis.

- A cost effective Sol Gel route can be employed for synthesis of zinc oxide nanorods.
- A capping agent is necessary for the formation and arresting the growth of nanorods.
- ZnO nanorods synthesized with Ethylenediamine as a capping agent, and calcinated at 150°C for 5 hours are approximately 300nm in length and have an aspect ratio of 3.75.
- The nanosized zinc hydroxide, upon calcination is completely oxidized to form zinc oxide nanorods.
- ZnO nanorods synthesized with Citric Acid Monohydrate as a capping agent exhibits calcination-temperature controlled morphology:

    - When calcinated at 170°C for 12 hours, nanorods are produced with an average length of 300 nm, and whose aspect ratio is 5.
    - When calcinated at 150°C for 12 hours, the amount of nanorods was reduced considerably. Nanostructures of various morphologies such as nanospheres, nanosheets, and undefined agglomerates were formed.
    - When calcinated at 125°C, the formation of nanorods is completely stopped, instead, agglomerates of near perfect nanospheres are observed. The size of such nanospheres is 200nm (dia) and the size of the agglomerates of the nanospheres is 800nm (dia) approximately.

- ZnO nanorods, when synthesized with Ethylenediamine as a capping agent, showed selective bactericidal activity against Gram negative *Escherichia coli* ATCC 25922 but no such activity was observed against Gram Positive *Micrococcus leuteus.*

- ZnO nanorods, when synthesized with Citric Acid Monohydrate as a capping agent, showed selective bactericidal activity against Gram positive *Bacillus subtilis*, but no such activity was observed against Gram negative *Escherichia coli* ATCC 25922.
- The minimum inhibitory concentration of ZnO nanorods synthesized by Sol Gel route is determined as:

    - ZnO dissolved in Water - **1.33** mg/ml
    - ZnO dissolved in Methanol - **0.332** mg/ml

FUTURE SCOPE

Nanorods of zinc oxide synthesized via a sol gel mechanism retain their morphology as well as bactericidal activity. The selective toxicity of the nanorods is controlled by the capping agent involved in the process. This can be considered as an added advantage and further antibacterial applications can be realized. The experimental work in this can be effectively utilized for:

Investigating the biochemical mechanism of bactericidal activity against susceptible strains, with a closer look on the surface interactions. Application of powders of such nanorods to artefacts and public places (public restrooms, open garbages etc.) and examine the activity in real time situations.

Coating of these nanorods to commonly touched/accessed places such as taps, handle rods in buses and trains, railings of staircases, where the transfer of harmful bacteria commonly occurs, and examining the antibacterial activity and effect of such nanorods.

REFRENCES

1. O. Yamamoto (2001), Influence of particle size on the antibacterial activity of zinc oxide, International Journal of Inorganic Materials, Vol. 3, pp. 643–646.
2. L. Zhang, Y. Jiang, Y. Ding, M. Povey, D. York (2007), Investigation into the antibacterial behaviour of suspensions of ZnO nanoparticles (ZnO nanofluids), Journal of Nanoparticle Research, Vol. 9, 479–489.
3. H.H. Sandstead (1994), Understanding zinc—recent observations and interpretations, Journal of Laboratory and Clinical Medicine Vol. 124, 322–327.
4. L. Zhang, Y. Ding, M. Povey, D. York, (2008), Prog. Nat. Sci. Vol. 18, 939.
5. J. Yang, X. Liu, L. Yang, Y. Wang, Y. Zhang, J. Lang, M. Gao, B. Feng, (2009), Journal of Alloys and Compounds, Vol. 477, 632.
6. P.-C. Kao, S.-Y. Chu, B.-J. Li, J.-W. Chang, H.-H. Huang, Y.-C. Fang, R.-C. Chang, (2009), J. Alloys Compd. Vol. 467, 342.
7. G. Guo, C. Shi, D. Tao, W. Qian, D. Han, (2009) J. Alloys Compd. Vol. 472, 343.
8. R.M. Trommer, A.K. Alves, C.P. Bergmann, (2010), J. Alloys Compd. Vol. 491, 296.
9. P. Huang, X. Zhang, J. Wei, B. Feng, (2010), J. Alloys Compd. Vol. 489, 614.
10. M.S. Mohajerani, A. Lak,. Simchi, (2009) J. Alloys Compd. Vol. 485, 616.
11. M. Mazloumi, S. Taghavi, H. Arami, S. Zanganesh, A. Kajbafvala, M.R. Shayegh, S.K. Sadrnezhaad, (2009) J. Alloys Compd. Vol. 468, 303.
12. N. Jones, B. Ray, K.T. Ranjit, A.C. Manna, (2008) Antibacterial activity of ZnO nanoparticle suspensions on a broad spectrum of microorganisms, FEMS Microbiology Letters, Vol. 279, 71–76.
13. K.H. Tam, A.B. Djurišić , C.M.N. Chan , Y.Y. Xi , C.W. Tse , Y.H. Leung , W.K. Chan , F.C.C. Leung , D.W.T., (2008), Antibacterial activity of ZnO nanorods prepared by a hydrothermal method. Thin Solid Films Vol. 516, 6167–6174.
14. S. Balaji, V. Prabhawathi, P.M. Sivakumar, R. Neelakandan, P.T. Manoharan, M. Doble, (2010) Effective antibacterial adhesive coating on cotton fabric using ZnO nanorods and chalcone. Carbohydrate Polymers Vol. 79, 717–723.

15. Moriarty P. (2001), Nanostructured materials. Rep Prog Phys; Vol. 64(3):297–381.
16. Nel A, Xia T, Madler L, Li N. (2006), Toxic potential of materials at the nanolevel. Science; Vol. 311(5761), 622–6277.
17. Toral D. Zaveri, Natalia V. Dolgova, Byung Hwan Chu, Jiyeon Lee, Joey Wong, Tanmay P. Lele, Fan Ren, Benjamin G. Keselowsky, (2010) Contributions of surface topography and cytotoxicity to the macrophage response to zinc oxide nanorods Biomaterials Vol. 31, 2999–3007.
18. J. Yang, X. Liu, L. Yang, Y. Wang, Y. Zhang, J. Lang, M. Gao, B. Feng, (2009), J. Alloys Compd. Vol. 477 , 632.
19. P.-C. Kao, S.-Y. Chu, B.-J. Li, J.-W. Chang, H.-H. Huang, Y.-C. Fang, R.-C. Chang, (2009), J. Alloys Compd. Vol. 467, 342.
20. G. Guo, C. Shi, D. Tao, W. Qian, D. Han, (2009) J. Alloys Compd. Vol. 472, 343.
21. R.M. Trommer, A.K. Alves, C.P. Bergmann, (2010) J. Alloys Compd. Vol. 491, 296.
22. P. Huang, X. Zhang, J. Wei, B. Feng, (2010) J. Alloys Compd. Vol. 489, 614.
23. M.S. Mohajerani, A. Lak,. Simchi, (2009) J. Alloys Compd. Vol. 485, 616.
24. C.-H. Lu, Y.-C. Lai, R.B. Kale, (2009) J. Alloys Compd. Vol. 477, 523.
25. M. Mazloumi, S. Taghavi, H. Arami, S. Zanganesh, A. Kajbafvala, M.R. Shayegh, S.K. Sadrnezhaad, (2009) J. Alloys Compd. Vol. 468, 303.
26. C. Karunakaran, V. Rajeswari, P. Gomathisankar (2010), Antibacterial and photocatalytic activities of sonochemically prepared ZnO and Ag–ZnO. Journal of Alloys and Compounds Vol. 508, 587–591.
27. ZnO nanofluids: Green synthesis, characterization, and antibacterial activity Contributions of surface topography and cytotoxicity to the macrophage response to zinc oxide nanorods Toral D. Zaveri, Natalia V. Dolgova, Byung Hwan Chu, Jiyeon Lee, Joey Wong , Tanmay P. Lele , Fan Ren , Benjamin G. Keselowsky
28. L.E. Greene, M. Law, D.H. Tan, M. Montano, J. Goldberger, G. Somorjai, P. Yang, (2005) Nano Lett. Vol. 5, 1231.

29. M. Law, L.E. Greene, J.C. Johnson, R. Saykally, P. Yang, (2005) Nature Mater. Vol. 4 455.
30. L.E. Greene, M. Law, J. Goldberger, F. Kim, J.C. Johnson, Y. Zhang, R.J. Saykally, P. Yang, Angew. (2003) Chem., Int. Ed. Engl. Vol. 42, 3031.
31. D. Li, Y.H. Leung, A.B. Djurišić, Z.T. Liu, M.H. Xie, S.L. Shi, S.J. Xu, W.K. Chan, (2004) Appl. Phys. Lett. 85, 1601.
32. A.B. Djurišić, M.N. Chan, Y.Y. Xi, K.H. Tam, C.W. Tse, Y.H. Leung, W.K. Chan, F.C.C. Leung, D.W.T. Au., (2008) Antibacterial activity of ZnO nanorods prepared by a hydrothermal method Thin Solid Films. Vol. 516, 6167–6174.
33. Jun Zhang, Lingdong Sun, Jialu Yin, Huilan Su, Chun Sheng Liao, Chunhua Yan, (2002) Control of ZnO morphology via a simple solution route, Chem. Mater. Vol. 14, 4172–4177.
34. Lubomir Spanhel, Marc A. Anderson J. (1991), Semiconductor clusters in the sol–gel process: quantized aggregation, gelation, and crystal growth in concentrated ZnO colloids, Am. Chem. Soc. Vol. 113, 2826–2833.
35. Ralph M. Nyffenegger, Ben Craft, Mohammed Shaaban, Sasha Gorer, George Erley, Rignald M. Penner, (1998), A hybrid electrochemical/chemical synthesis of zinc oxide nanoparticles and optically intrinsic thin films, Chem. Mater. Vol. 10, 1120–1129.
36. C.J. Brinker, G.W. Scherer, (1990) The Physics and Chemistry of Sol–Gel Processing, Sol–Gel Science: Academic Press, San Deigo.
37. M.K. Hossain, S.C. Ghosh, Y. Bootongkang, C. Thanachayanont, J. Dutta, (2005) Growth of zinc oxide nanowires and nanobelts for gas sensing, J. Metastable Nanocryst. Mater. Vol. 23, 27–30.
38. Laudise, E. D. Kolb, A. J. Caporaso, (1964), J. Am. Ceram. Soc. R. Vol. A, 47, 9.
39. M. Suscavage, M. Harris, D. Bliss, P. Yip, S. Q. Wang, D. Schwall, L. Bouthillette, J. Bailey, M. Callahan, D. C. Look, D. C. Reynolds, R. L. Jones, C. W. Litton, (1999) MRS Internet , J. Nitride Semicond. Res., Vol. 4S1, G3.40.
40. Wen Jun Li, Er Wei Shi, Tsuguo Fukuda, (2003), Particle size of powder under hydrothermal conditions, Cryst. Res. Technol. Vol. 38, 847–858.

41. Hui Zhang, Deren Yang, Xiangyang Ma, Yujie Ji, Jin Xu, Duanlin Que, (2004) Synthesis of flower-like ZnO nanostructures by an organic-free hydrothermal process, Nanotechnology Vol. 15, 622–626.
42. Chung Hsin Lu, Chi Hsien Yeh, (2000) Influence of hydrothermal conditions on the morphology and particle size of zinc oxide powder, Ceram. Int. Vol. 26, 351–357.
43. Tsuzuki T and McCormick P, (2001) Scripta mater. Vol. 44, 1731– 1734.
44. Ding J, Tsuzuki T and McCormick P G, (1997) Nanostruct. Mater., vol.8, 75.
45. Tsuzuki T, Mccormick P G, (2000) Acta mater. Vol. 48, 2795-2801.
46. P.M. Sivakumar, S. Balaji, V. Prabhawathi, R. Neelakandan, P.T. Manoharan, M. Doble, (2010) Effective antibacterial adhesive coating on cotton fabric using ZnO nanorods and chalcone. Carbohydrate Polymers Vol. 79, 717–723.
47. J. Apachitei, Duszczyk, L. Katgerman, and P.J.B. Overkamp, (1998) Scripta Materialia. vol. 38, pp. 1383.
48. A. Srivastava, S. Mohan and V. Agarwala and R. C. Agarwala, (1992) Z. Metallkunde. vol. 83, pp. 251.
49. N. Jones, B. Ray, K.T. Ranjit, A.C. Manna, (2008) FEMS Microbiol. Lett. Vol. 279, pp. 71.
50. G. Applerot, A. Lipovsky, R. Dror, N. Perkas, Y. Nitzan, R. Lubart, A. Gedanken, (2009) Adv. Funct. Mater. Vol. 19, 842.
51. Nina Perkas, Galina Amirian, Olga Girshevitz, Aharon Gedanken, Guy Applerot, (2009) Coating of glass with ZnO via ultrasonic irradiation and a study of its antibacterial properties, Applied Surface Science Vol. 256S, S3–S8.
52. J Sawai, T. Yoshikawa, (2004) Quantitative evaluation of antifungal activity of metallic oxide powders (MgO, CaO and ZnO) by an indirect conductimetric assay, J. Appl. Microbiol. Vol. 96, 803–809.
53. Ken Hirota, Maiko Sugimoto, Masaki Kato, Kazuhiko Tsukagoshi, Tooru Tanigawa, Hiroshi Sugimoto, (2010) Preparation of zinc oxide ceramics with a sustainable antibacterial activity under dark conditions Ceramics International. Vol. 36, 497–506.

54. K.H. Tam, A.B. Djurišić, M.N. Chan, Y.Y. Xi, C.W. Tse, Y.H. Leung, W.K. Chan, F.C.C. Leung, D.W.T. Au., (2008) Antibacterial activity of ZnO nanorods prepared by a hydrothermal method Thin Solid Films. Vol. 516, 6167–6174.

55. R. Neelakandan, P.M. Sivakumar, S. Balaji, V. Prabhawathi, P.T. Manoharan, M. Doble, (2010) Effective antibacterial adhesive coating on cotton fabric using ZnO nanorods and chalcone. Carbohydrate Polymers Vol. 79, 717–723.

56. Tamar Gordona, Benny Perlsteina, Ofir Houbarab, Israel Felnerc, Ehud Baninb, Shlom Margela, (2011) Synthesis and characterization of zinc/iron oxide composite nanoparticles and their antibacterial properties. Colloids and Surfaces A: Physicochem. Eng. Aspects. Vol. 374, 1–8.

57. J. Sawai, (2003) J. Microbiol. Methods Vol. 54, 177.

58. F. Furno, K.S. Morley, B. Wong, B.L. Sharp, P.L. Arnold, S.M. Howdle, R. Bayston, P.D. Brown, P.D. Winship, H.J. Reid, (2004) J. Antimicrob. Chemother. Vol. 54, pp. 1019.

59. N. Ciofi, L. Torsi, N. Ditaranto, L. Sabatini, P.G. Zambonin, G. Tantillo, L. Ghibelli, M. D'Alessio, T. Bleve-Zacheo, E. Traversa, (2004) Appl. Phys. Lett. 85, pp. 2417.

60. N. Ciofi, L. Torsi, N. Ditaranto, G. Tantillo, L. Ghibelli, L. Sabatini, T. Bleve-Zacheo, M. D'Alessio, P.G. Zambonin, E. Traversa, (2005) Chem. Mater. Vol. 17, pp. 5255.

61. Razieh Jalal, Elaheh K. Goharshadia, Maryam Abareshia, Majid Moosavic, Abbas Yousefid, Paul Nancarrowe,(2010) ZnO nanofluids: Green synthesis, characterization, and antibacterial activity. Materials Chemistry and Physics Vol. 121, 198–201

62. Rizwan Wahab, S.G. Ansari, Young-Soon Kim, Hyung-Kee Seo, Hyung-Shik Shin, (2007) Room temperature synthesis of needle-shaped ZnO nanorods via sonochemical Method, Appl. Surf. Sci. Vol. 253, 7622–7626.

63. N. Padmavathy, R. Vijayaraghvan, Sci. Technol. (2008) Adv. Mater. Vol. 9, pp.035004

64. G. Applerot, A. Lipovsky, R. Dror, N. Perkas, Y. Nitzan, R. Lubart, A. Gedanken, (2009) Adv. Funct. Mater. 19, pp. 842.

65. Deepali Sharma, Jaspreet Rajput, B.S. Kaith, Mohinder Kaur, Sapna Sharma, (2010) Synthesis of ZnO nanoparticles and study of their antibacterial and antifungal properties Thin Solid Films Vol. 519, 1224–1229.
66. Guy Applerot, Nina Perkas, Galina Amirian, Olga Girshevitz, Aharon Gedanken, (2009) Coating of glass with ZnO via ultrasonic irradiation and a study of its antibacterial properties. Applied Surface Science 256S, S3–S8.